Reconstructing extreme discharge events

A case study applying LOI for core-to-core validation of flood event registration

Date of submission:	February 7, 2010
Author:	Tiuri Konijnendijk, BSc.
Student number:	0423947
Supervisor:	dr. Kim Cohen
Institute:	Department of Physical Geography Faculty of Geosciences Utrecht University

Universiteit Utrecht

Abstract

In this explorative study, four cores from three closely spaced infilled-channel sites are analyzed to investigate the reproducibility of flood event registration in fluvial-deltaic environments. The influence of channel fill architecture, i.e. the effect of position of the core in a residual channel, is examined. The application of Loss On Ignition (LOI) – applicability, reliability, and optimal methodology – is investigated. The aim is to establish an event layer correlation between the obtained cores within one residual channel in both longitudinal and lateral direction and deliver proof of the concept of cross correlation of flood event records between these sites.

Fieldwork was carried out near the apex of the Rhine-Meuse delta (Waalprong, Nijmegen). Paleogeographic maps pinpoint the residual channel locations. Four cores were retrieved from a residual channel and brought to the Utrecht University laboratory for subsampling and analysis. For 1267 subsamples (12.7m of core material) LOI was measured, for 255 subsamples also carbonate content was determined. Explorative statistics were applied to the acquired data in order to obtain the desired information. Three types of computerized analyses are described in this study. One is the influence of possible disturbing factors. Another is the effect of lower resolution LOI sampling on data quality. Finally, the cross correlation, or wiggle matching, of the extracted cores.

The cores are found to have filled in rapidly, with relatively clastic material. An average weight percentage of carbonates of 20% is found, and organic matter fluctuates between 1-10%. Infilling proceeded the most in the deepest cores. Carbonates show a strong but erratic relationship with LOI outcomes. No clear influence of carbonate content, or sample position in the furnace, on LOI reliability is found. Long drying times before furnace processing are found to have a negative impact on LOI result. Modeling of lower sampling resolutions yields good results up to 3cm resolution sampling, after which data deterioration is too great. The optimal resolution for other records may be different, based on the length of the investigated record. The cross correlation of cores in this rapid-aggradation setting proves to be very well possible using LOI data. The used approach, whereby the data was first smoothed by a running average window, allowing focus on longer lived trends before fine tuning short lived events, was successful. All four cores were successfully wiggle matched. This supports the use of LOI for flood event registration and the practice of correlating flood event records using wiggle matching.

Contents

Figures

Tables

1. Introduction

1.1 research techniques for investigating flood events

This thesis results from an exploration of some of the aspects of paleoflood event research. In this study, cores from several closely spaced sites were analyzed to investigate the role of these aspects for flood event research. The aim was to i) examine the influence of channel fill architecture, i.e. the effect of position of the core in a residual channel ii) explore the application of Loss On Ignition (LOI) – applicability, reliability, and optimal methodology – on this research iii) establish the inter-core relations within one residual channel in both longitudinal and lateral direction and deliver proof of the concept of cross correlation of flood event records.

Fieldwork was carried out upstream in the Rhine-Meuse delta (figure 1.1). The area was mapped for paleogeographic reconstruction and pinpointing of residual channel locations. Four cores were retrieved from a residual channel and brought to the Utrecht University laboratory for analysis. These cores provide the material with which this research was executed. These cores were subsampled; subsamples were processed, and explorative statistics were applied to the resulting data in order to investigate the effects of channel fill architecture and LOI methodology. Finally, this information was shaped into synoptic imagery to enable analysis and allow conclusions to be drawn.

Figure 1.1: The Waalsprong fieldwork area. The grey rectangle indicates the fieldwork area for this study.

1.2 Background to flood event research

In 2007, Cohen and Lodder outlined a research approach to expand the current knowledge of the frequency and magnitude of past floods in the Rhine-Meuse delta, using paleogeographical data. Their purpose was a better understanding of the probability of experiencing extreme discharges (recurrence interval and magnitude) for flood safety in the delta today. Data extracted from the sedimentary archive should provide input for improved statistical calculation of recurrence intervals for extreme discharge events, as presently expected and usable for projected future situations (Cohen and Lodder, 2007).

Flood event research is still in an adolescent stage, and many aspects have uncertainties about them. In this thesis, effects of channel architecture and sampling procedures are explored to provide a foundation for flood event research to build on.

1.3 To be tested: Basic principles exploited in flood event research

Residual channels a small distance away from active channels contain records of flooding activity from surrounding active channels, based on the input of clastic material (Middelkoop 1997). During large flood events, relatively coarse material reaches the distal residual channels. During periods of low activity finer clastic sediment is deposited and possibly organic materials form. Over time the residual channel is gradually filled with a sequence of coarse and fine sediments. The proposed approach means to document incidents of coarse material and analyze the record of flood events once incorporated into a whole, continuous dataset (Cohen and Lodder, 2007).

The establishment of a flood event record and of a transcending dataset deltaic flooding history may prove to suffer from shortcomings. Possible flaws that may cause local flood event record quality deteriorate may come from too low sampling resolution, less than clear effect of changes in river activity, or problems with data reliability. Also, flood event research is based on some assumptions regarding the intercomparison of different records. Below is explained what these assumptions are and how they are tested in this research.

A basic assumption underlying the idea of composing a master dataset of flood records is the idea that it is possible to cross correlate individually registered events from different cores and, for the largest events, even from different channel fills. Flood events in a local record will be matched to events registered in records from other locations, based (inter alia) on resemblance in the variation between these records. The research design is fortified by the fact that flood event recognition and characterization is a multi-proxy affair, and supported by markers – archeological, ecological, chemical events of influence – as well as ^{14}C and pollen datings.

This study, after investigating the reliability of LOI, uses the LOI data to test this principle in a case study. The limited distance between the cores in this study makes it likely that cross-correlation of event layers in the cores is possible. In the process, computer analyses are performed to investigate what would be the best methodoloty for LOI in flood event research.

1.4 Outline of this thesis

Chapter 2 first provides basic information regarding channel fill architecture and sediment composition. Also, the use of LOI on flood event records is explained. In chapter 3, the selection of the fieldwork area and the residual channel in it is presented. Chapter 4 describes the sampling procedures applied to the cores and the laboratory analyses. Chapter 5 provides details of the exploratory statistical analyses that were performed on the laboratory results, as well as their outcomes. Chapter 6 discusses the consequences of the results obtained in chapter 5. Chapter 7 summarizes the conclusions drawn from this study. Chapter 8 contains recommendations for future channel fill research.

2. The analysis of channel fills: theory

2.1: The residual channel as a record

Knowledge of the mechanisms responsible for filling in residual channels is vital to finding the best spot for taking the cores in this study targeted at flood reconstruction. Box 1 illustrates the build-up of a residual channel record. The stages involved can be discerned on basis of the material: grain size and sorting, amount of organic material, the type of organic remains involved, etc.

Box 1: the stages of residual channel filling

When a river abandons a channel, flow velocity decreases and sediment is deposited in the (now residual) channel. The process of infilling can be divided into several stages.

A) Active stage: flow and sediment load are more or less in equilibrium, no net deposition of sediment.

B) Abandoning stage: the river activity changes, (bulk of) the discharge takes place over a different route. This may occur quickly, such as with a meander cut-off, but it can also take longer before abandonment is complete. For instance, from the onset of abandonment (the start of avulsion) to its completion (i.e. complete infilling of the residual channel) an average of 400 years is recorded (Stouthamer, 2001). During abandoning, there is too much sediment load for the reduced flow to transport, and net deposition of sediment occurs, especially at the 'entrance' of the channel (paragraph 2.2.2)

C) Abandoned stage: little or no flow persists through the residual channel. Only limited clastic material is depositioned in the residual channel. The channel may be slowly filled in by the formation of organic material, alternated with clastic laminae deposited during flood events.. For a very deep channel this infilling process may take thousands of years (Minderhoud, 2008).

D) Buried stage: the residual channel has become completely filled in and no more open water remains.

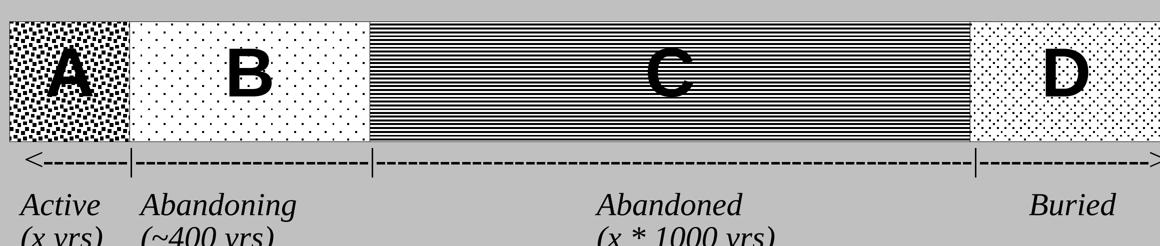

Figure 2.1: schematic display of different stages of infilling over time.

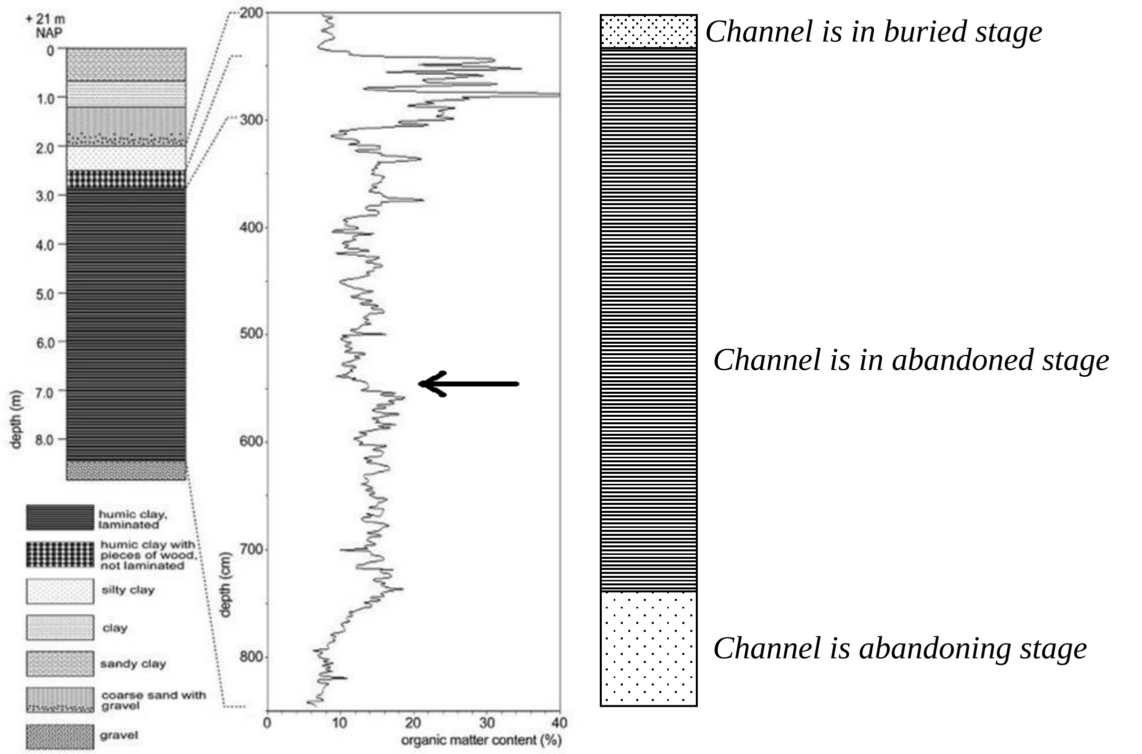

Figure 2.2 stages in residual channel filling of a channel fill (after Minderhoud, 2008). The stages of infilling are displayed alongside. The black arrow indicates a shift in background sedimentation rate.

In the example of the Rheinberg core of Minderhoud (2008; figure 2.2), the bottom part is characterized by a steady build-up of organic material in the deposits. This is characteristic for decreasing flow velocities while the channel is abandoned. At a depth of 7.40 m below the surface, the organic material reaches a more or less constant background level of organic matter/clastic material associated with gradual infilling of the residual channel in the abandoned stage. The deposition rate decreases and remains relatively constant. About half way in this stage, a shift occurs in the background level of the organic matter content. This indicates a change in clastic input from the active channel, probably it means the channel shifts to a more proximal position. From 3.15 m below the surface, the residual channel is filled so that the limited water depth allows for plants and trees to grow; organic matter content increases. At 2.40 m below the surface the residual channel is completely filled up, peat formation stops and all depositions from that point are clastic material during flooding activity.

2.2 Channel fill architecture

Research into the architecture of channel fills was performed by IJmker (2008). This study details the lateral and longitudinal infilling of a residual channel during and after abandonment. This information is relevant for finding the best spot for obtaining a sediment record, which is usually the deepest point of a residual channel. The deepest point, where before abandonment the thalweg ought to have been, is the target location for obtaining cores. There are thee advantages to the deepest point. Primarily, it provides the most accommodation space for residual channel deposits, thereby rendering the most extensive records. Secondly, in the channel infill scenarios discussed in the previous chapter, the deepest point suffers the least disturbances by the process of channel narrowing. Thirdly, at the bottom, channel lag deposits topped by clayey deposits indicate sudden avulsion, whereas a channel lag topped by sand may simply indicate the toe of a scroll bar and provides less information.

Considering cross channel architecture, IJmker divides the filling in of a residual channel into two processes: narrowing and shallowing. These processes are important in the next subparagraph concerning lateral variation in channel fills. After this, longitudinal variation in channel fills is discussed. Differences in stratigraphy of a channel fill as a consequence of position in longitudinal sense plays an important role in reconstructing the paleogeographic setting based on stratigraphy, as is attempted in this research.

2.2.1 Lateral variation in channel fills

IJmker (2008) developed three end member scenarios that explain the processes channel narrowing and shallowing that take place in residual channels. These scenarios are displayed in figure 2.3.

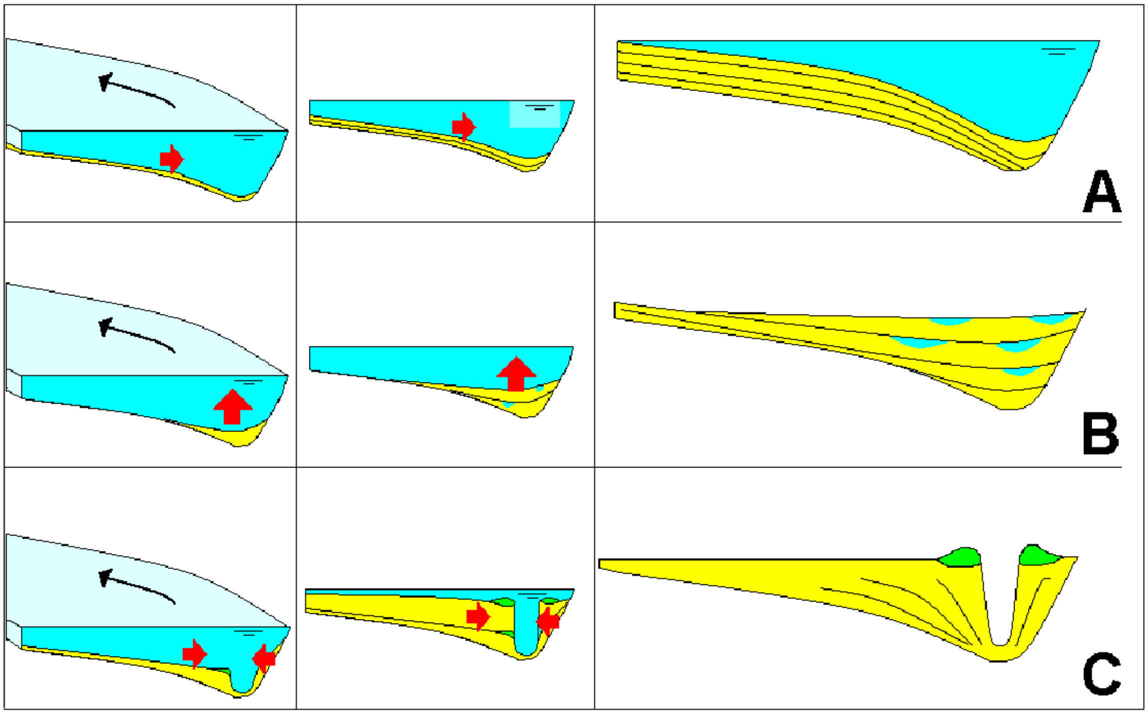

Figure 2.3: Cross-sections of possible scenarios for residual channel fills in a meander bend. Black arrows indicate the main flow direction, red arrows indicate the direction of bank and bed accretion (after: IJmker, 2008).

In scenario A ("lateral outward"), erosion of the outer bend will be limited due to decreasing flow velocities after channel abandonment. Meanwhile the deposition in the inner bend and channel lag continues. This results in both narrowing and shallowing of the channel. The scenario assumes sand transport in the channel despite decreasing flow velocities. This scenario is possibly recognized by an extensive sand body at the lower side and at the inner bend of the channel.

This situation is most likely to occur in straighter sections of a residual channel, downstream of the abandonment point. Here, residual flow is not as concentrated as in a bend, allowing for deposition in the channel lag as well as on the sides of the channel.

In scenario B ("channel wide shallowing") the silting up is characterized by channel wide shallowing. According to IJmker (2008), this is most likely when the sediments are not (strongly) cohesive and the high sediment load causes a braided pattern. An abundance of several smaller channel deposits in a large sand body would testify for this scenario. Small channels can be represented by coarser sediments or, in case of inactive periods, clay drapes.

The high accumulation rate is explained by high deposition rates as a result of an abrupt decrease in flow velocity. This is likely to occur at or near the abandonment point, where a ‘plug bar’ is formed after an avulsion takes place. See the next subparagraph for more information on plug bars.

In scenario C (“narrowing with preservation of depth”), channel the process is dominated by channel narrowing. Predominantly cohesive sediments are deposited along the residual channel, especially but not exclusively at the inner bend. This type of situation is most likely under circumstances with a slow flow velocity decrease, a high clay content, and low sand content. Particularly in bends, downstream of the abandonment point, where flow is concentrated. In that case a narrow, deep channel will develop.

Such a channel fill can be recognised by a narrow channel with possibly the formation of levee deposits. Levee deposits result from flooding and thus this scenario requires a relatively long avulsion duration: long enough for several significant flood events. To have been conveyed through the abandoned channel, the deposits in the steady formed banks possibly show a fining trend towards the final channel.

According to IJmker (2008), the channel fill architecture varies with the rate of discharge decrease, the composition of the transported sediments and other factors. These factors may well vary with position in the residual channel, both in longitudinal and lateral sense. This means that different scenarios may be dominant along the channel. This is better illustrated in the next subparagraph.

2.2.2 Longitudinal variation in channel fills

In figure 2.4 three scenarios for longitudinal channel fill architecture depending on avulsion duration are presented. A long avulsion duration implies slow abandonment of a residual channel (scenario 1). This results in a long period of sand transport, after which the residual channel is eventually filled with finer materials. The opposite end member of IJmker (2008) occurs when a sand plug is formed at the upstream inlet. The channel is rapidly closed and rarely allows discharge, only at very high water levels (scenario 3). In this scenario, a long ‘abandoned’ period with organic matter deposition is more likely in this scenario. The second scenario presents an intermediate situation; a decrease in flow velocity that results in a slow succession of finer clastic sediments.

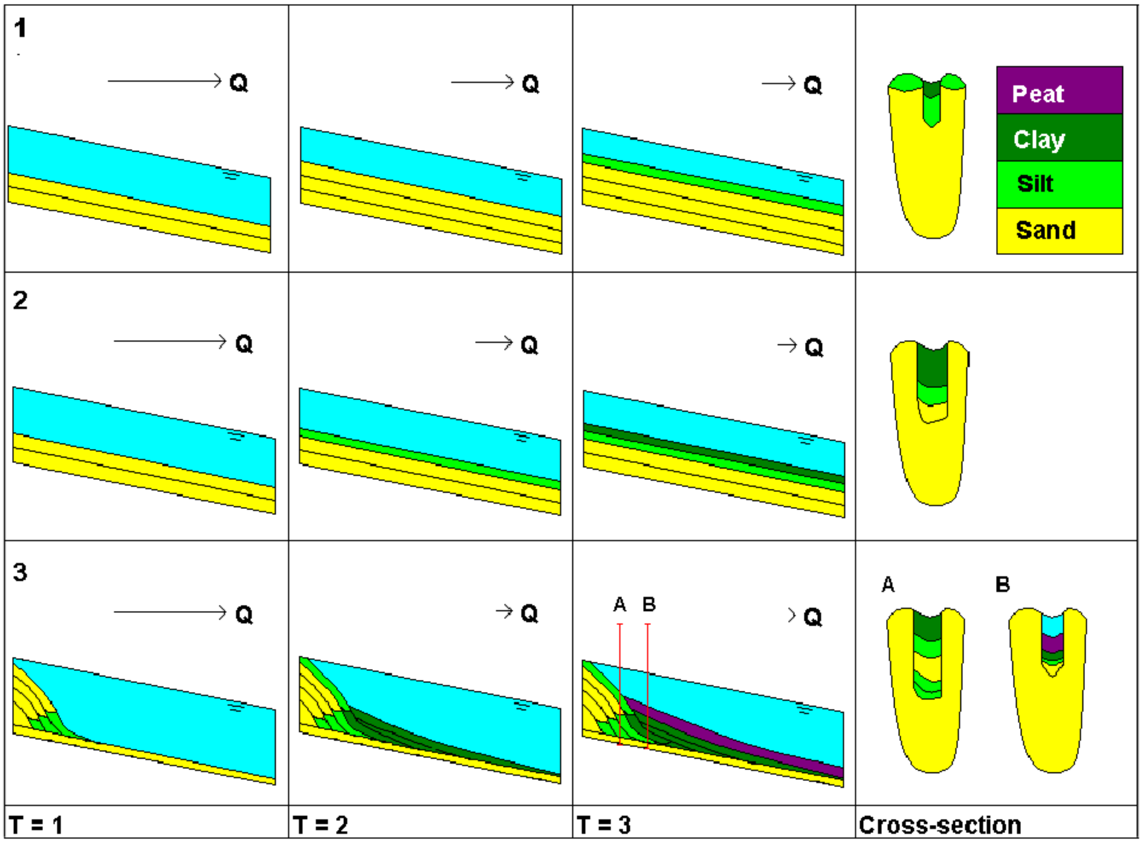

Figure 2.4: Variation in longitudinal channel fill architecture with avulsion duration. Scenario 1 represents long avulsion duration; scenario 3 represents short avulsion duration. Scenario 2 is an intermediate scenario. The arrow length is an indication for (decrease of) flow velocity. Note that the slope is exaggerated (after: IJmker, 2008).

These scenarios represent ideal situations, unlikely to occur exactly as presented here. The development of the residual channel fill strongly depends on the activity and proximity of the active channel. Therefore, the channel filling can differ in downstream direction, depending on distance to the abandonment point and the distance to the active system. For instance, the influence of individual flood events is smaller or absent further away from the active system. Also, the infill is influenced by local factors in the residual channel. The width of the channel influences the local flow characteristics, which can increase or decrease sedimentation.

2.3 The application of LOI on channel fill analysis

2.3.1 Clastic input and its effect on LOI

The LOI method is used to measure the amount of organic material in weight percentages of a sample. Its methodology is discussed in chapter 4. The input of more clastic material during flood events will reduce the relative contribution of organic material in a sample. Therefore, a flood event will be indicated by a short lived drop in LOI (figure 2.5).

Apart from single events, represented by short lived drops in the LOI curve, there exists a background signal in the clastic input in the residual channel as described in section 2.1. The amount of influence of the active channel on the deposits in the residual channel depends on several factors. One is the activity of the active channel itself. Another is the distance between the residual channel and the active system. A third is the ease with which water reaches the residual channel during floods. This depends, for instance, on the existence and dimensions of a plug bar, and on properties (such as vegetation cover) of the terrain separating the residual channel from the active channel. The influence of these factors on the subject matter of this research will be discussed in chapter 6.

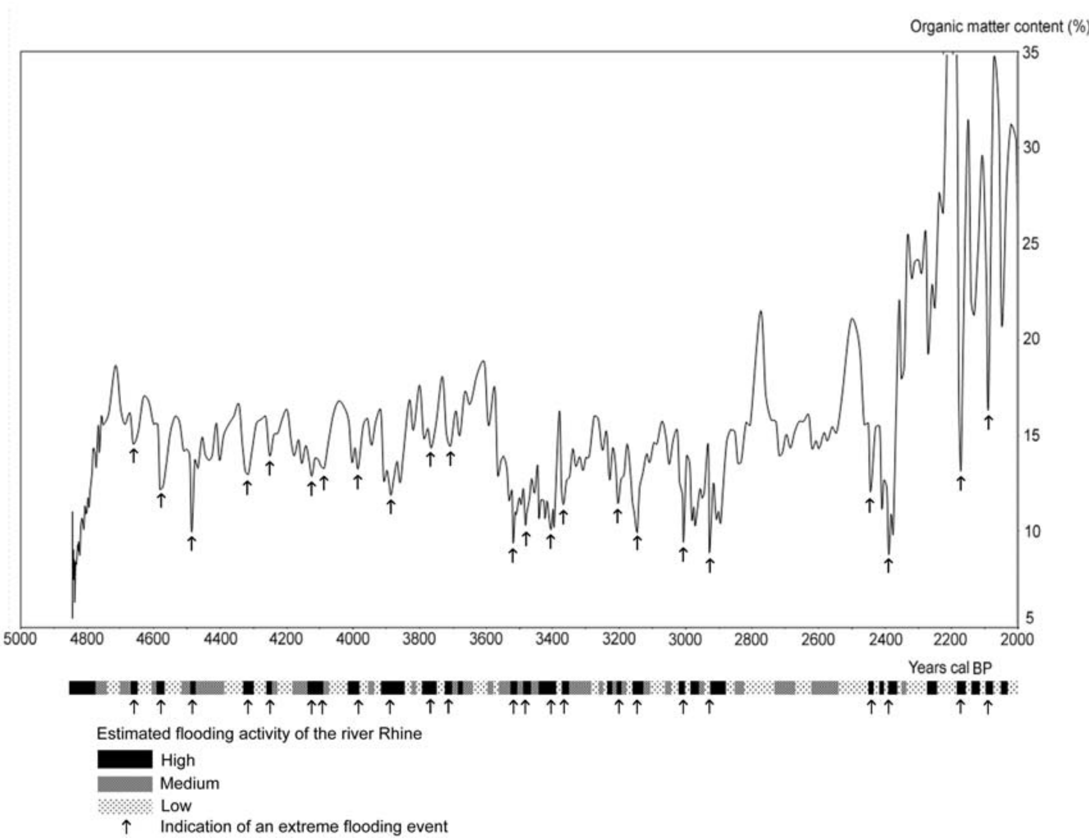

Figure 2.5: finding flood events in a sedimentary record using LOI. A drop in the curve indicates a flood event. Arrows mark sections with high clastic input (after Minderhoud, (2008).

2.3.2 The correlation of several cores

For all four of the cores that were extracted during fieldwork an LOI curve, similar to that of figure 2.5, was produced. Each curve has a different average LOI value and consists of different material, i.e. more clastic, coarser, different amounts of shell fragments etc. This, as well as local influences on deposition, make it impossible to simply 'count from the top' the amount of clastic layers in each core to derive the flooding history of the area. The inter-core differences are simply too great to arrive at a satisfactory conclusion.

Yet, the curves ought to resemble each other enough to allow cross-correlation of the data. Any attempt to establish a regional flooding history depends on this. Moreover, the possibility of interconnecting large scale changes in local records allows maximizing these signals and minimizing noise from local factors, according to the principle of replication (described in chapter 1).

To start the process of interconnecting data, or 'wiggle matching', one needs markers that tie certain points in each core to each other. Regional influences that provide detectable and constricted changes in the sediment, which occur simultaneously in all cores, e.g. an ash layer from a forest fire. Additionally, to allow cross correlation of very thin strata data between individual cores, a certain amount of similarity in the depositional environment is required. In the obtained cores, little no such markers have been found during this research. Pollen data provides far too general information to use as a marker on this timescale (10^1-10^2 years). Instead, since all cores in this research are derived from the same residual channel, the only marker used was the channel lag. Sedimentation was assumed to start simultaneously from that point in all cores. The rest of the cross correlation process was done via wiggle matching, which will be explained in detail in chapter 5.

3. Acquisition of the cores

A suitable site was selected for the research as part of the larger campaign (see also chapter 1). Special attention was given to the selection of the exact locations for core extraction. Cores were taken using both hand and machine operated piston corers described below, and transported to Utrecht for subsampling and laboratory analysis.

Site selection for fieldwork was based on the availability of river Rhine paleochannels, suitability of terrain for coring, and prospective results for the obtained cores. The required knowledge to judge possible locations was derived from previous coring operations and the high resolution elevation model for the Netherlands, the AHN (Rijkswaterstaat – AGI, 2005). Preexisting coring data was found in the delta-wide LLG database of the dept. of Physical Geography (Berendsen, 2005) and local investigations of the RAAP. The selected site, namely the Waalsprong area, and its corresponding features are described below.

Next, the fieldwork process is discussed. The procedure used to determine the exact location of residual channels is recounted. After that, the materials used for coring are described and the treatment of the obtained cores in the field is explained.

3.1 Waalsprong fieldwork area

3.1.1 Residual channels in the Waalsprong area

The Waalsprong area is located to the north of the city Nijmegen in the province of Gelderland (figure 1.1). Throughout the Holocene, the river Rhine has flowed in this area, replacing most of the preexistent Pleistocene terrace deposits with channel bed and flood plain deposits of meandering rivers.

The position of the main, water carrying channel has shifted many times by processes of meandering, as well as avulsion. In the geomorphological-geological map of the Rhine-Meuse Delta (Berendsen and Stouthamer, 2001) the deposits of meandering rivers in the area have been attributed to Ressen channel belt complex. A local reconstruction of Rhine channel belt activity in the area has been produced by Lodiers (2008 – internship Gem. Nijmegen report).

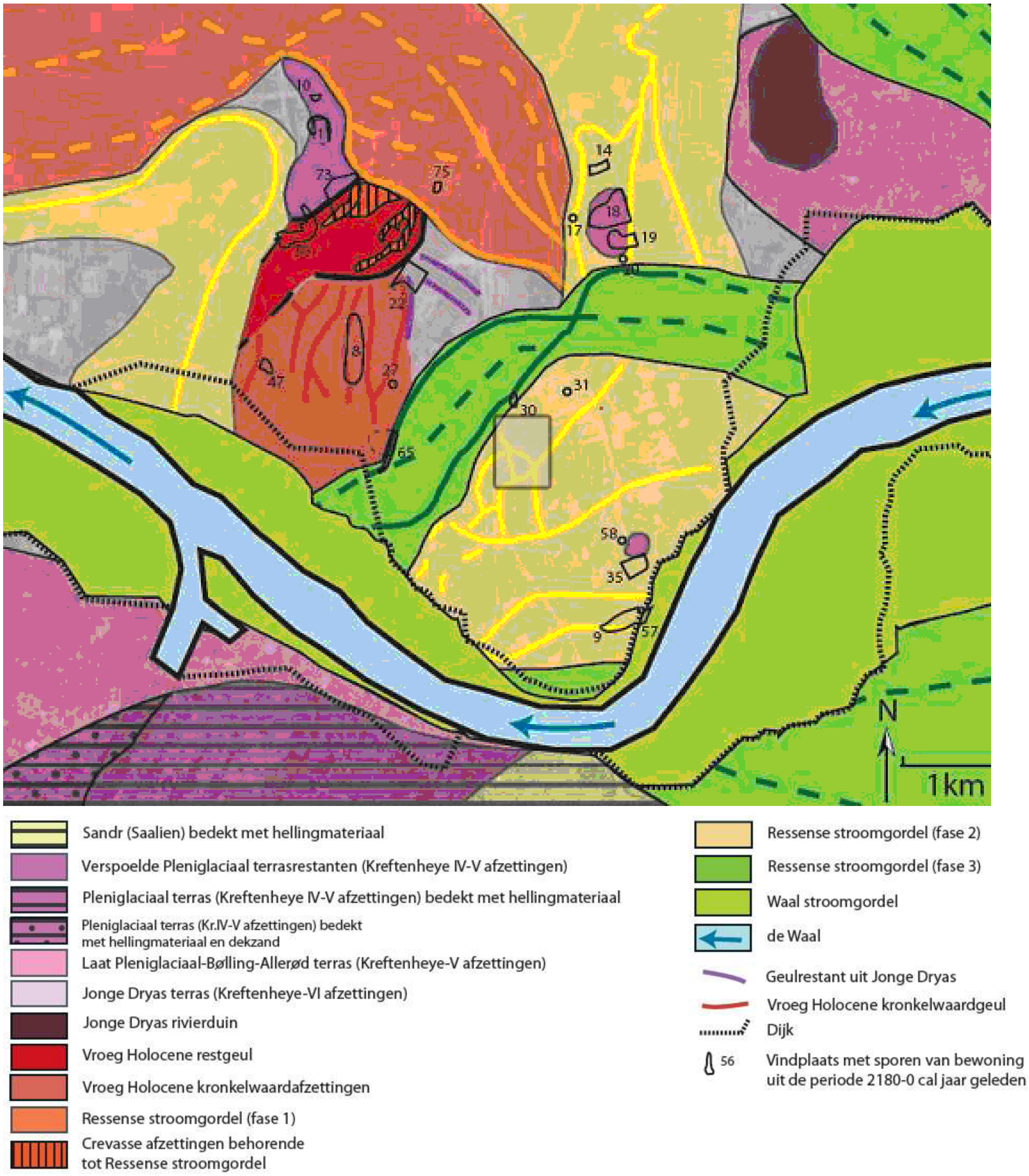

Figure 3.1: Palaeogeographic map of the current situation in the Waalsprong area (Lodiers, 2008). The grey rectangle indicates the fieldwork site for this study.

This work subdivides the Holocene history in 5 phases. On the resulting palaeogeographical map (figure 3.1), fragments of Pleistocene terrace and Early Holocene deposits are separated by Middle and Late Holocene channel belt deposits, mainly from the phases ~4500-3000 cal years BP, 3000-2180 cal years BP and the 2180-present position of the Waal. The Middle and Late Holocene deposits each contain several residual channels (figure 3.1).

3.1.2 Recognizing and selecting residual channel sites

A residual channel may be recognized by its characteristic morphology. A residual channel that is buried is often still visible as a longitudinal depression in the landscape that is usually curved (in the case of a meandering paleochannel). The depression is caused by relatively stronger compaction of the clay and peat in a residual channel, compared to the coarser clastic material of the surrounding banks and channel belt (Berendsen and Stouthamer, 2001).

Making use of the detailed elevation model AHN, such depressions may be recognized as areas of interest prior to fieldwork. In addition, earlier research has yielded data on where to find residual channels. Multiple residual channels are found in each of the phases of the Waalsprong area (figure 3.1). Also, exploratory corings in the Waalsprong area extracted from the University of Utrecht LLG database (Berendsen, 2005) and the RAAP provide information about the sediments at specific points. This may point to the existence (or absence) of a residual channel at certain locations as well.

During fieldwork in the Waalsprong area, hand performed corings supply the proof for the existence of residual channels. The exact location of residual channels may be mapped by documenting sedimentological aspects of the subsurface. When coring a cross section, the typical sequence found is fine clastic material, rich in organic matter, often in a banded or layered pattern in the residual channel, bordered by coarser clastic material in the surrounding channel belt.

Over 20 different locations in the Waalsprong area were explored during fieldwork. This involved distinct residual channels from different phases in the Ressen channel belt complex, but also multiple locations along the same residual channel were explored.

For this research, a channel was selected from the available locations in the Waalsprong area. This specific channel allowed acquisition of several closely spaced cores, both in cross channel and along channel direction, ideal for this research. It is located in Lent, in an empty stretch east of the N325 motorway. This stretch was actively studied by archeologists at the time of the fieldwork and the banks of the channel, which were inhabited during Roman times.

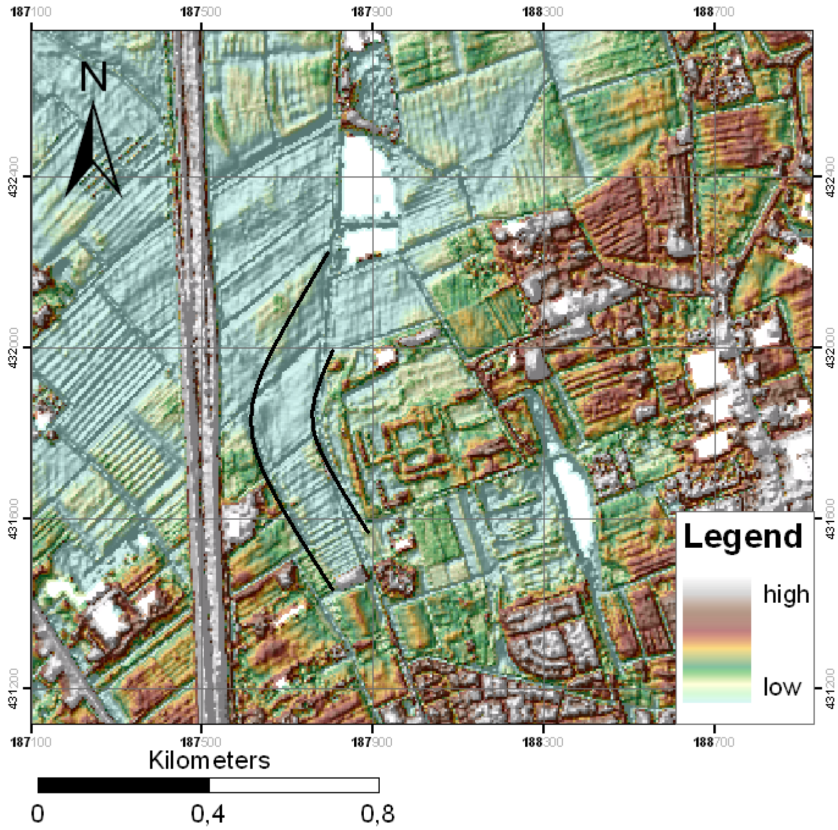

Figure 3.2: AHN image of the fieldwork site. Black lines underline the limits of the paleochannel.

The channel position is clearly visible in the AHN image of the area (figure 3.2), and is located just south of the centre of the fieldwork area. According to the work of Lodiers (2008) this channel formed in the second phase of the Ressen system. This implies this system was active ~4500-3000 yrs BP. After abandonment, an active system stretching east-west north of the abandoned channel acted as source of the infilling material (figure 3.1).

In addition to the AHN data, records of previous corings performed by Utrecht University (Berendsen, 2005) and RAAP sand depth records of the Waalsprong (RAAP, 2001) yielded locations where probable or confirmed residual channel deposits had been found.

3.2 Fieldwork procedures

3.2.1 Site verification: procedure and results

Using hand operated coring devices the fieldwork area was probed, with the objective to find the boundaries of the residual channel and its deepest point. During the hand coring expedition, corings were performed along cross channel transects. Each transect is usually delimited by corings in the sandy channel belt deposits. In the central part of each transects, hand corings are closely spaced, sometimes only 10 m apart. Two transects are placed at different sites along the paleochannel (figure 3.4). The southern transect (transect 1) location was chosen based on a 1992 coring from the LLG database (Berendsen, 2005). The northern transect (transect 2) was placed based on the AHN image and location (adequate distance) relative to the other transects. In the middle, at the location of core c, corings were added to an earlier transect by Cohen and Heunks (pers. comm.), which already gave a quite detailed display of the residual channel (figure 3.3), was extended.

Error! Objects cannot be created from editing field codes.

Figure 3.3: existing cross section of the residual channel based on an earlier transect by Cohen and Heunks (pers. comm.)

The results were processed into cross sectional images, which are attached at the end of this thesis (appendices 1 a, b, c). Also, the purvey knowledge served to determine the sites for extraction of the cores upon which this research is based. This resulted in the extraction of 4 cores (a-d), at locations indicated in figure 3.4. Further information about the cores is given in table 3.1.

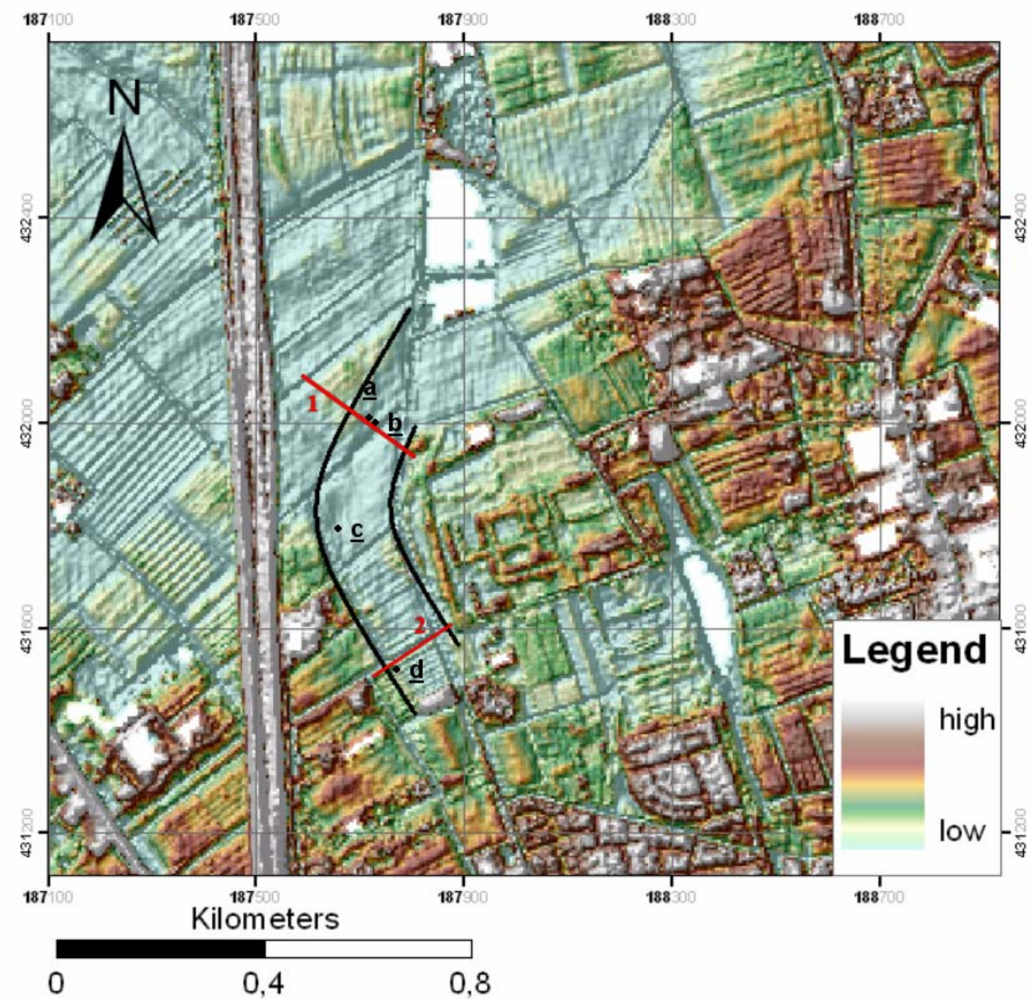

Figure 3.4: location of the extracted cores. Coring locations are indicated with black dots, accompanied by an identifying letter. Red lines indicate cross sections.

Core	location (RD)	LLG database id	surface level (m)	core depth (cm)	name
a[1]	187726, 431996	200905045	9.10	550	6 diep Visveld Noord
b[1]	187736, 431985	200905042	8.88	500	6 ondiep Visveld Noord
c[1]	187665, 431779	200905057	9.18	782	5 Visveld Midden
d[2]	187778, 431502	200905050	9,30	500	7 Lent Graveyard

Table 3.1: specification of the extracted cores. The cores indicated by the number 1 are extracted using the Begemann corer (see below for further information). The core indicated by the number 2 was extracted using hand operated material.

3.2.2 Prospective coring with hand operated coring materials

The explorative hand corings were performed using the common Edelman corer. This is standard practice in geomorphological research on the Rhine Meuse Delta at the Quaternary geology research group of the UU (see also their website, referred to under coring methods. This simple device (figure 3.3) is operated by one person who drives it into the ground by twisting the T-shaped handles. It can be extended extension using additional 1 m extension pieces and often easily penetrates any material (sand, peat, clay) above ground water level. Sampling occurs every 10 cm.

Figure 3.5a: prospection coring material (after: www.eikelkamp.nl)

Figure 3.5b: Example of sampling with the simple hand gauge (after: coring methods)

After reaching ground water level, the Edelman corer is exchanged for more suitable gear, depending on the encountered ground material. In clay or peat below ground water level it is best to use the gauge (figure 3.5a; figure 3.5b), which enables extraction of 80 cm each thrust. In sandy material, the van der Staay suction corer (Van de Meene et al., 1979) is used. This device enables extraction of several meters (3m, 5m, or more) at once.

Using these materials, a pair of researchers can perform 6 corings of 5 meters' depth, covering a moderately large transect in high detail, in less than a day.

3.2.3 Extracting sediment cores with hand operated material

The Bohncke hand operated piston corer (modified Livingstone piston corer; W.Z. Hoek, Utrecht University) is a device of medium complexity that can be used by a team of 3 persons to extract cores from a given site. It performs poorly in sandy material, which jams its moving components, but renders good results in peat and clay. If properly operated, it produces 1 m segments of a core with a diameter of 8 cm, with relatively undisturbed material in the centre of the core. The latter is important in the case of laminated residual channel deposits. An additional advantage is that virtually any site accessible on foot may be subject to use of the Bohncke corer, due to its relatively low weight and small amount of parts that need to be transported.

The corer is dropped to a previously cored hole to groundwater level. The inner rod is retracted 1 meter, leaving the hollow outer tube, with a cutting edge, in place. Next, the whole device is pushed down, forcing material in the empty outer tube. Once the full device is retracted from the borehole, the inner rod is used to push the core segments out of the outer tube and onto 1 m half-pipe segments, which protect the core material.

The cores are wrapped in plastic foil, covered by half pipe lids, and again wrapped in foil and a plastic sack for optimal protection against physical disturbances and oxidation during transport and storage. The reopening and processing of these cores is described in the next chapter.

3.2.4 Materials: extracting cores with the Begemann mechanical corer

The Begemann mechanical corer (Deltares, 2009) is a small caterpillar truck that can be drove to location and set to extract cores of up to 20 m depth. Though able to navigate difficult terrain, its applicability is restricted to locations with limited relief.

Figure 3.6a: picture of the Begemann steel outer barrel with cutting edge (after: Deltares 2009)

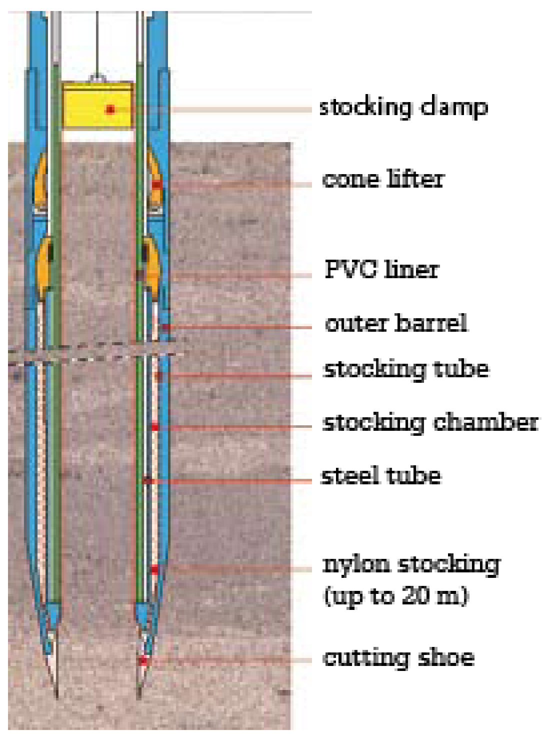

Figure 3.6b: schematic display of the Begemann mechanical corer (after: Deltares 2009)

The Begemann mechanical corer drives a double tube into the ground with a force of up to 13 tons, thereby far surpassing the coring capabilities of any hand operated core. Additionally, it contains no moving parts and this, in combination with its power, enables coring through any loose sediment, including moderate gravel. When applied to residual channels, it creates a continuous core from surface to channel lag. Because of the simplicity of the process, delicate laminated deposits are undisturbed, giving the Begemann advantage over e.g. the Vibracorer. Its construction is made up of two tubes. The first is a steel outer barrel with a sharp cutting edge at the bottom (figure 3.6a). This is forced down, bringing the core material into the inner tube. The inner tube consists of PVC pipe (figure 3.6b). Its outside is lined with stocking, which is pulled around the core material by the movement of the core.

As the corer is forced into the ground, this creates a continuous PVC pipe, with core material wrapped in stocking on the inside. When the corer reaches the channel lag deposits this is marked by a sharp increase in pressure required to force the corer down. The process is halted, and the corer is brought up. At every meter interval, the core and inner tube are cut, and top and bottom sides are capped to close the core for transport and storage. The reopening and processing of these cores is described in the next chapter.

4. Core sampling and processing of subsamples

This chapter explains how the cores are treated after acquisition: the opening process, procedures applied prior to sampling, the sampling process, and laboratory analyses on the subsamples.

4.1 Opening and sampling

To open a core, it is cut in half over its entire length. Next, it is photographed following a standard protocol. Then, a visual assessment is recorded of each core. After this recording and assessing of the intact core, one half is wrapped for storage and the other used for sampling.

4.1.1 Opening a core

Two types of core were handled: Bohncke cores and Begemann cores. The opening procedure is quite similar, except for the beginning.

In case of a Bohncke core, the core material is wrapped in plastic foil and covered by two half pipe lids. After removing one lid and opening the plastic wrap, the core is cut with a thin steel thread. The core is turned along its longitudinal axis and the two halves are carefully separated. Each laid in a separate half pipe for further treatment.

In the case of a Begemann core, the top and bottom caps need to be removed from the PVC tube that contains a core. A half pipe is readied, and the core is pulled from the PVC tube and laid into a half pipe. The stocking is removed, and afterwards the treatment is identical to that of Bohncke core segments.

After the two halves are placed next to each other, measuring tape is used to confirm the core's length. The tape is placed between the halves with the tick marks up and at the correct place (i.e. top and bottom of the core at their corresponding tick marks). Then, pictures are taken at set intervals to document the core's appearance digitally.

Figure 4.1: example of a panoramic picture of core c, segment AIV

The digital pictures are combined, in this case using the freeware computer program 'Autostitch' (Brown and Lowe, 2007). This program uses overlap in photographs to create one panoramic picture out of separate photos (e.g. figure 4.1). The results of the combined pictures are found in appendix 2.

Once the photographs are taken, a visual assessment of the core's attributes is made. All distinguishable features are documented. This includes lithology, lamination, color and color differences, appearance of e.g. siderite, shell fragments, charcoal and plant remains, as well as signs of oxidation, bioturbation, and other disturbances. The resulting description of each core is found in appendix 2. After photography and visual assessment, one half core is wrapped in plastic foil for long term refrigerated storage. The other is sampled, as described in the next subparagraph.

4.1.2 Sampling

During the sampling activities a standard protocol was followed. The subject half core was placed with the bottom side left, and sampled from left to right at 1 cm resolution. Two incisions were made 1 cm apart over the entire length of the half core with a simple cutting utensil. In case of sampling for LOI as well as carbonate measurements, a third incision was added another 1 cm apart. Each of these incisions was about 1 cm deep.

Next, at every tick mark on the measuring tape, a cross length incision is made in the material between the earlier cuts. This results in 1 x 1 cm cubes that are only attached to the half core at their bottom. With the help of a small gauge these cubes are extricated and placed in the appropriate crucible or phial, depending on the analysis.

The total of all cores sampled has surmounted to 1267 samples used for LOI. Samples were generally just under 1 cm^3 in size, with an average bulk weight of 1.4 g, and a standard deviation of 0.25 g.

In addition, 255 samples of unspecified size were taken for carbonate measurements. In the later analyses discussed in chapter 5, these carbonate samples are regarded as the corresponding LOI sample. Because they come from the same depth as their LOI twin, it is simpler to add a carbonate content value to samples that are tested for both.

The total of carbonate samples taken is limited, because the use of the carbonate measurements is mainly to investigate how they affect LOI measurements. Therefore, only the cores a and c were sampled, partially.

Generally, sampling for LOI measurements was started immediately above the channel lag deposits in each core. Sampling was stopped when laminations and other details disappear or are too disturbed, usually at the ground water level, because of oxidation, bioturbation, and iron oxide precipitation.

In some cases sampling was difficult, such as with very unstable, disturbed material when large wood fragments appeared in the core. When this occurred, sampling was sometimes passed over. Also, sometimes the recorded top and bottom depth of adjacent core segments did not correspond in the case of the Bohncke core. In these cases, and when sampling was passed over, their corresponding crucibles or phials were left empty for the remaining analyses.

In addition to the described samples for laboratory testing, samples were taken for pollen counts. These samples were taken from core a at every 35 cm or on lithological boundaries within cores. The pollen data generates information on sedimentary environment and potentially provides age constraints to the sediments (Middelkoop, 1997). Pollen preparation and analysis were outsourced to a different laboratory (TNO). The results are discussed as part of the data integration in chapter 6.

4.2 Protocols for laboratory analyses

4.2.1 Carbonate measurements

For carbonate measurements, each sample extricated from a core is put into a plastic phial with an open top. The phials are put in a stove at 70 °C to dry for 24 hrs. The dried samples are ground to dust and a fraction of about 0.3 grams is used for carbonate measurements using the Scheibler apparatus (Petersen et al., 1966).

The Scheibler apparatus exploits the reaction of soil carbonates when exposed to hydrochloric acid. This reaction produces a volume of CO_2 which is proportional to the amount of soil carbonates, assuming all carbonates dissolve in a large amount of acid. The volume of gas that is produced is measured using the apparatus.

The exact weight percentage of carbonates in a sample can be determined when the required factors are known, namely: weight of total sample, volume of CO_2 gas produced, and volumetric production rate of CO_2 gas per gram of carbonate. The latter depends on local air pressure, and is determined each 4 hours with a Scheibler test on pure carbonates prior to sample testing.

A complete and accurate description of the principles and practice of volumetric carbonate content quantification can be found in Petersen et al., 1966.

4.2.2 LOI measurements

For the Loss On Ignition method of determining organic matter content (Dean, 1974), a range of protocols is in use. An attempt to standardize the LOI protocol was made by Heiri et al. (2001). Their proposed protocol has been followed during this research and will be briefly described below.

Subsamples are put in open crucibles of 1.5 x 3 cm and their bulk weight is measured to $1*10^{-3}$ g accuracy. The weight of the crucible, measured beforehand, is deducted to obtain sample bulk weight. Samples are dried for a period of 24 hrs (or more) at 105 °C, and sample dry weight is measured. The difference constitutes sample water content, which is assumed to be responsible for the total of weight loss in this time.

After drying, samples are placed in a furnace and heated to 550 °C for 4 hrs. Note that Heiri et al. (2001) propose 4.5 hrs of ignition time. This research was conducted using 4 hrs of ignition time because it saves some time every day. The difference ought not to influence the outcome of LOI measurements because: 1) the samples are still exposed to temperatures above 300 °C for several hours while the furnace cools down, and 2) the study of Heiri et al. shows a sharp decrease in weight loss rate after 4 hrs of ignition time (figure 4.2).

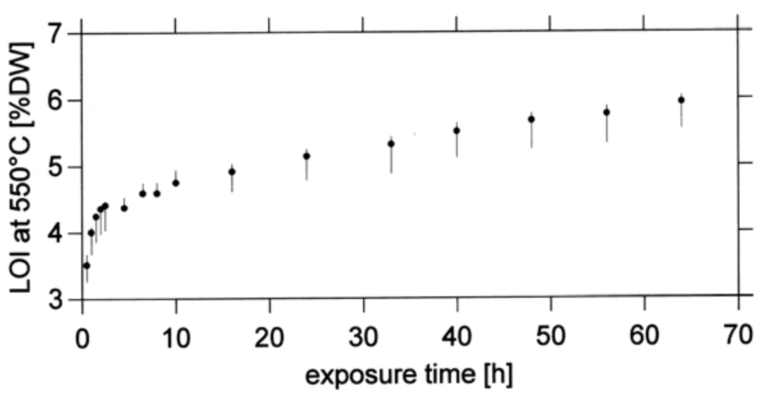

Figure 4.2: weight loss late of samples in the furnace. After 4 hours of exposure to 550°, the weight loss rate sharply declines (after Heiri et al., 2001)

After cooling for 3 hours, the batch is removed from the furnace and the sample remains are weighed. The weight loss of the sample is completely attributed to combustion of organic carbon during ignition time in the furnace. The weight difference between sample dry weight and final weight is divided by the sample's dry weight to obtain a weight percentage of organic matter.

Values for LOI during this research typically ranged between 1 - 10%. That puts the core materials in the range of normal to humic clays or sands. No sensu stricto peat samples have been found based on these values, as peat by formal definition (De Bakker and Schelling, 1966) has an LOI value of 30% or more.

It was found that occasional presence of relatively large plant remains in samples does not significantly affect LOI measurements. Subsamples with visible fragments of organic matter did typically not have a visually higher LOI value than their direct neighbors without visible fragments of organic matter. Such remains in samples were therefore ignored for the rest of the conducted analyses.

5. Results and analysis of datasets

The laboratory analyses yielded results on the organic matter and carbonate content of the samples which are presented in this chapter. The generated data has been used in a number of additional, computerized, analyses in order to shape meaningful information out of dry data. A description is given of the several performed analyses and the approach they took.

In the first paragraph, the basic, unprocessed findings of the fieldwork and performed laboratory measurements are given. Next, the testing of the reliability of this data is presented. The third paragraph covers the analyses performed to find the optimal signal/noise ratio. Finally, the process of cross correlating the data from different cores is described. The spread sheet model used for wiggle matching the cores and its results are presented.

5.1 Description of cores and laboratory data

In this paragraph the unprocessed data on the core is presented. Basic information on each core's lithology is provided, and the LOI and carbonate measurement data is displayed. Table 5.1 gives an overview of the performed measurements.

core	**core depth (m)**	**LOI measurements**	**$CaCO_3$ measurements**
a	5,50	5,32m - 2,67m (267 subsamples)	5,32m - 4,15m (118 subsamples)
b	5,00	4,85m - 2,05m (277 subsamples)	-
c	7,82	7,70m - 3,61m (410 subsamples)	7,70, - 6,91m (80 subsamples)
d	4,97	4,97m - 1,95m (300 subsamples)	-

Table 5.1: overview of the performed measurements

5.1.1 Core a

Core a is the northernmost core, positioned in the deepest point of the residual channel. It is 5.50m deep, divided into 7 segments. It consists primarily of fine clastic material and has visible laminae over most of its length (appendix 2 a). The bottom of the core consists of coarse, clastic material, which is classified as channel lag deposits. The sudden transition between these deposits and finer sediments indicates a quick conversion from active to residual channel, at a point upstream of the location of this core.

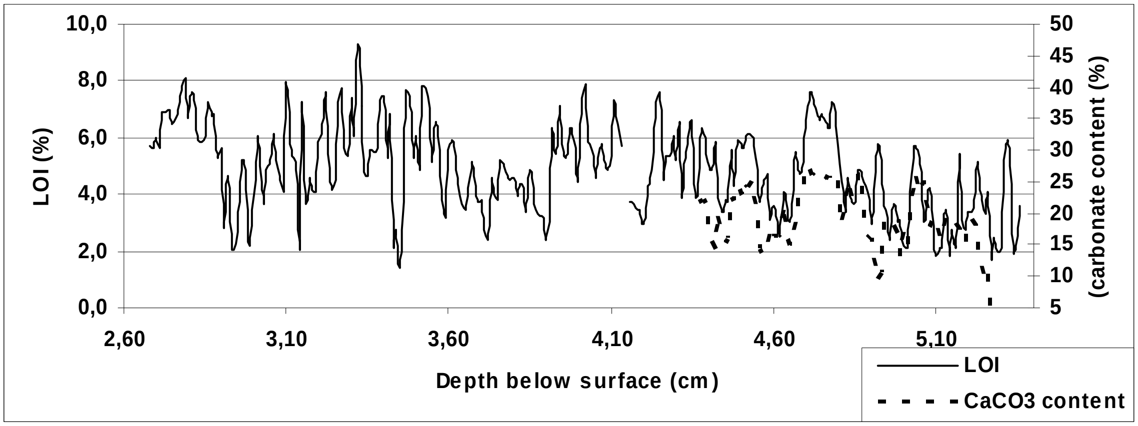

Figure 5.1 LOI and carbonate results for core a. Carbonate content is scaled on the secondary y-axis

The core was subsampled for LOI from the channel lag deposits, 5.32m below the surface, up to 2.67m below the surface, resulting in 267 subsamples. Additionally, subsamples were taken for carbonate measurements from the channel lag deposits up to 4,15m below the surface (118 samples). Above 2.67m increasing oxidation and bioturbation of the sediments prevented further subsampling. The LOI and carbonate measurements are both highly variable (figure 5.1)

5.1.2 Core b

Core b is located just southwest of core a, positioned 25m away from the deepest point of the residual channel, in the direction of the outer bend. This core is 5.00m deep and is divided in 7 segments. Similar to core a, the bottom of this core consists of coarse (channel lag) deposits, with an abrupt transition to finer, laminated clastic sediments (appendix 2 b)

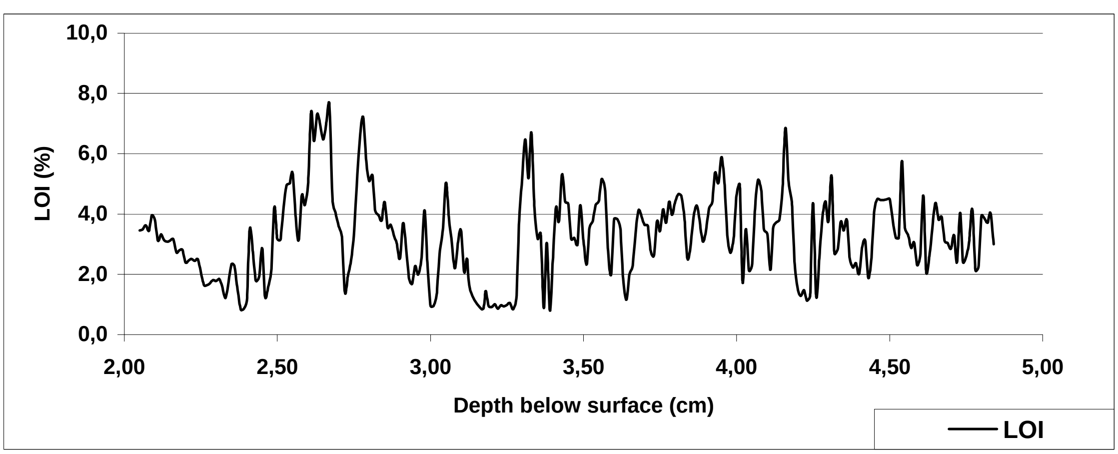

Figure 5.2: LOI results for core b

The core was subsampled for LOI measurements from 4.85m below the surface up to 2.05m below the surface, above which the material was completely oxidized and no laminae were visible. A total of 277 subsamples were analyzed resulting in a curve of the organic matter content (figure 5.2). No carbonate measurements were performed on the material from this core.

5.1.3 Core c

Core c is located over 200m south of core b, at the deepest point of the residual channel. The core is 7.50m deep, divided into 9 segments. The bottom contains gravel with pebbles. On top of these (channel lag) deposits, there is fine clastic, laminated sediment, with an occasional small pebble in the lowest 30cm. The transition is sharp, although less sharp than in cores a and b (appendix 2 c).

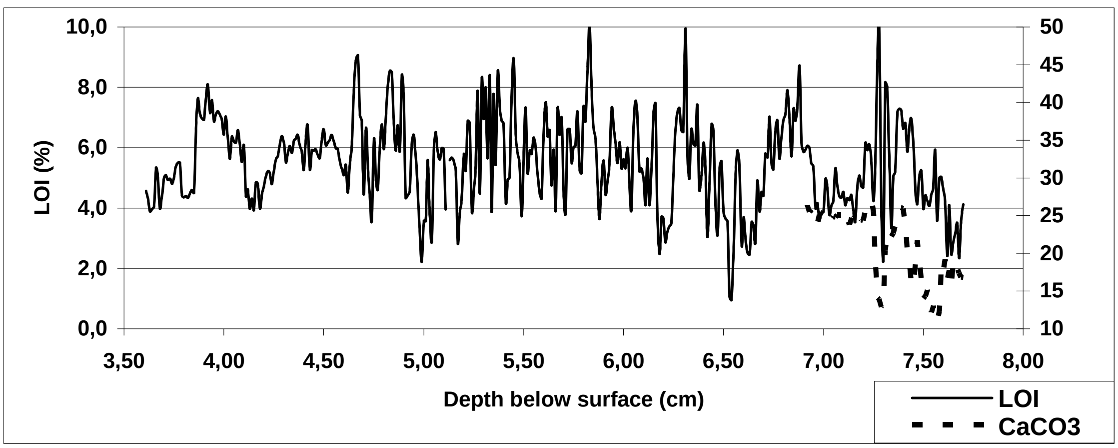

Figure 5.3 LOI and carbonate results for core c. Carbonate content is scaled on the secondary y-axis

The core was subsampled from the top of the channel lag deposits, at 7.70m below the surface, up to 3.61m below the surface for LOI. Above here bioturbation increased, and preliminary wiggle matching with the other data indicated that the overlap with the other datasets was already complete. The total dataset for this core comprises 410 LOI subsamples. Also, the bottom 80 cm (from the channel lag deposits up) was subsampled for carbonate measurements. The results are again highly variable, especially in the mid-section of the core (figure 5.3)

5.1.4 Core d

Core d is located an additional 300m southeast of core c. It is the only core that was obtained with hand operated coring materials, and the material was often slightly more disturbed than in the other cores. The core is 5m deep, divided into 4 segments. The sediments in this core were generally sandier than that of the other cores, ranging from clay to very fine silt, with more coarse but also more humic laminae. Coarse grains were not found on the bottom (appendix 2d), indicating the channel lag deposits were not reached or at least not penetrated with the piston corer. Therefore, while the start of the residual channel fill in the other cores was considered synchronized, the results from the bottom of this core was not.

Core d was subsampled from 4.97m below the surface, up to 1.95m below the surface for LOI, which coves the complete core. The local groundwater table was at 1.95m below the surface, limiting this hand operated corer's use. A total of 300 subsamples were analyzed, resulting in an organic matter content curve (figure 5.4).

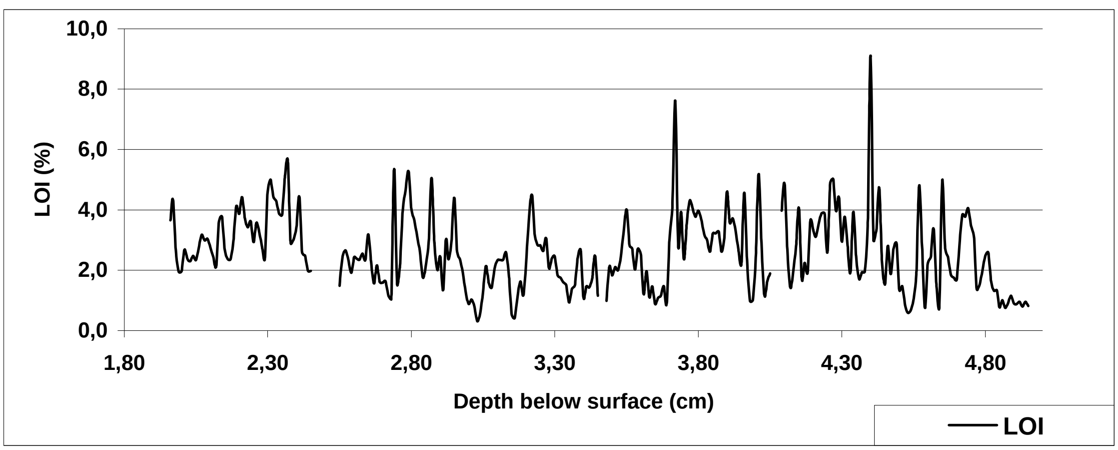

Figure 5.4: LOI results for core b

5.2 Reliability of data

The analyses described later in this chapter are all performed on the LOI data. An important factor to consider is the reliability of LOI data as a tool for flood event research. The LOI data exhibits much variability (e.g. figure 5.4), which could originates from measurement errors rather than differences in the sediments. In this paragraph, several possible influences on LOI measurements are identified.

5.2.1 Influence of carbonates on LOI

To investigate the influence of carbonates, 255 samples from two separate cores were tested both for LOI and carbonate content. An average weight percentage of 19.9% was found in the tested samples, with a standard deviation of 5.1%. No samples could be classified as very calcareous. Carbonate content, which is closely related to silt content, varied markedly through the record and showed a strong positive correlation with LOI (figure 5.5). Distinct divergences in the records are also visible at 6.30 m, 6.65 m, 7.30 m, and the interval 6.90-7.20 m depth.

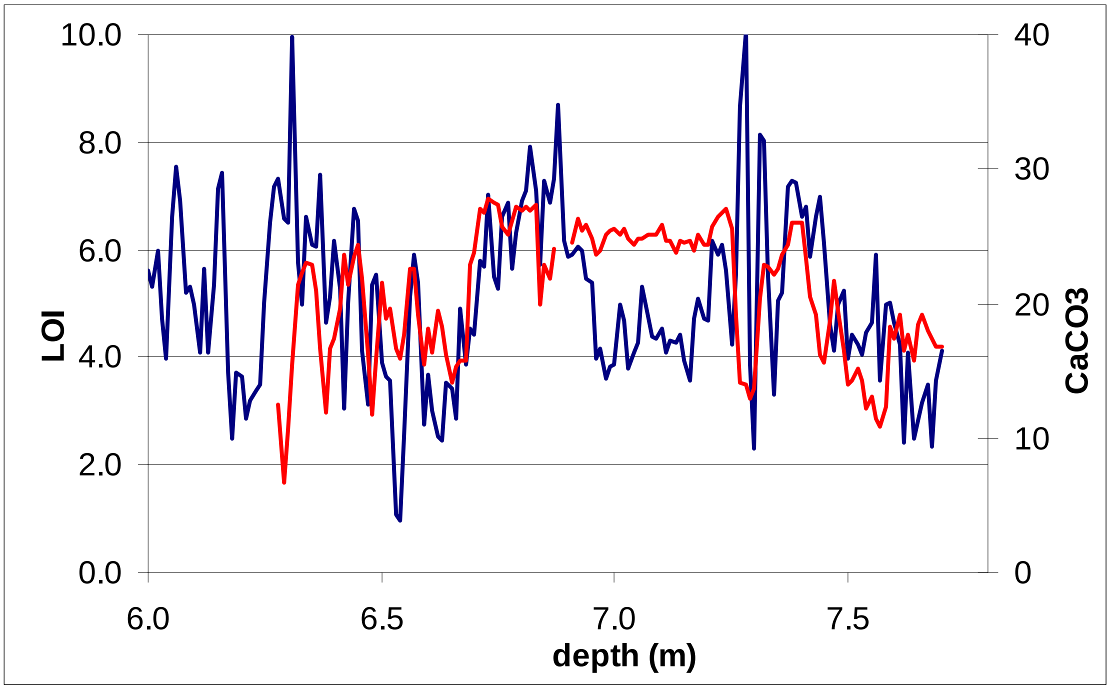

Figure 5.5: carbonate levels (red line) and partial LOI results (blue line) from core c.

The presence of carbonates may influence LOI result as aragonite and, on a smaller scale, calcite, partially ignite at 550 °C (Heiri et al, 2001: Duijkers, 2009). The LOI outcomes were compared to carbonate levels. Three classes were formed: samples with relatively low carbonate levels, samples with intermediate carbonate levels, and samples with relatively high carbonate levels.

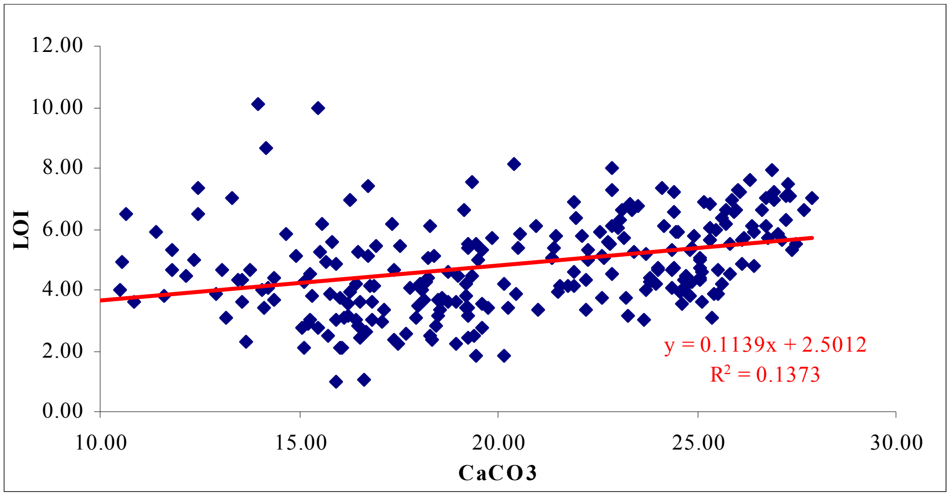

Figure 5.6: correlation between carbonate content and LOI results.

The LOI values of the samples in each class were compared to the average LOI value. Contrary to expectations, carbonate content did not appear to have any influence on a sample's LOI score (figure 5.6). The carbonate content of a sample does not significantly affect LOI results. This is reflected in the correlation graph (figure 5.6).

A possible explanation for this outcome is that the average carbonate content is quite low compared to the values in Heiri (2001) and Duijkers (2009). Also, it implies that the carbonate mostly consists of its more stable form, calcite, which requires a high temperature to combust (950 °C) and is less likely to be significantly affected at the 450 °C it is exposed to in this research.

5.2.2 Influence of furnace on LOI

The position of a sample in the furnace possibly influences the outcome of the LOI procedure (Heiri et al., 2001, Duijkers, 2009). Unequal heat distribution within the furnace or differences in oxygen levels are the cause for this discrepancy. This supposedly often results from slight defects in the furnace, such as a malfunctioning door leaking heat at the front side (Heiri, O.; pers. comm..).

The effect of furnace position was investigated while performing LOI analyses. The position of all samples was documented, and statistical analyses were performed on the resulting dataset. The furnace supports 25 crucibles, so samples can have 25 possible positions (figure 5.7a) a)

1	2	3	4	5
6	7	8	9	10
11	12	13	14	15
16	17	18	19	20
21	22	23	24	25

b)

3.9	4.2	3.9	4.1	4.0	Back
4.5	4.1	3.9	4.2	4.2	
4.2	4.0	4.4	4.6	4.9	
4.3	4.1	3.9	4.6	4.5	
3.7	3.7	3.8	4.0	4.2	Front

Figure 5.7 a) distribution of crucibles in furnace. Each number constitutes a possible position. b) average LOI value measured for all samples processed in that position. The positions are colour coded: relatively high values in red, intermediate values in orange, low values in yellow.

The dataset of 1267 LOI samples therefore generated near 50 samples for every possible position. Assumed was that each position coordinate supported populations of samples with roughly equal variation in organic material. Under perfect conditions, that should result in roughly equal LOI variation and mean as well.

The sample means for each position was calculated to find any obvious discrepancies in LOI as dependant variable of furnace position (figure 5.7b). There is variation in means between different positions, but there is no row or position that shows distinctly lower or higher values than the others.

This finding is supported by an F-test and subsequent student's T-test performed on positions 3 and 23 (mid-back and mid-front positions, respectively). An F-test was performed to test the statistical hypothesis of equal variances in both populations. The hypothesis was rejected, and a two-sample student's T-test assuming unequal variances was performed on the same data. This resulted in convincing acceptation of the hypothesis of equal means.

From both these tests and the results in figure 5.7b, the conclusion was drawn that the chance of significant differences in LOI results based on furnace influences are slim. If these influences exist, they are not appreciably affecting LOI results used for reconstructing flood events in channel fill records.

5.3.3: other influences on LOI

Similar to the tests performed on sample position on the furnace, a test was performed on the influence of drying time on LOI. Samples are dried for a period of 24 hrs minimum before placement in the furnace. In practice, cores were sampled before long term storage, resulting in 100 samples of approximately 1 cm^3. The furnace capacity allowed treatment of 50 samples per day (2 batches of 25).

This resulted in samples awaiting furnace treatment for periods longer than 24 hrs, sometimes over the weekend. The prolonged exposure of these samples to oxygen in a warm (105 °C) environment may have caused notable premature oxidization in some samples.

A test was run to find out the effect of prolonged drying time of samples on LOI. The time of each sample in the stove was documented. This period ranges between a period of 21 hrs (exceptional minimum) and 123 hrs (maximum end member). Again, each possible drying period is represented by at least one batch of 25 samples, and populations with roughly equal variation in organic material were assumed. Two approaches were taken to investigate the possible effect: all LOI values were plotted against drying time and a logarithmic relationship calculated based on the method of least squares (figure 5.8).

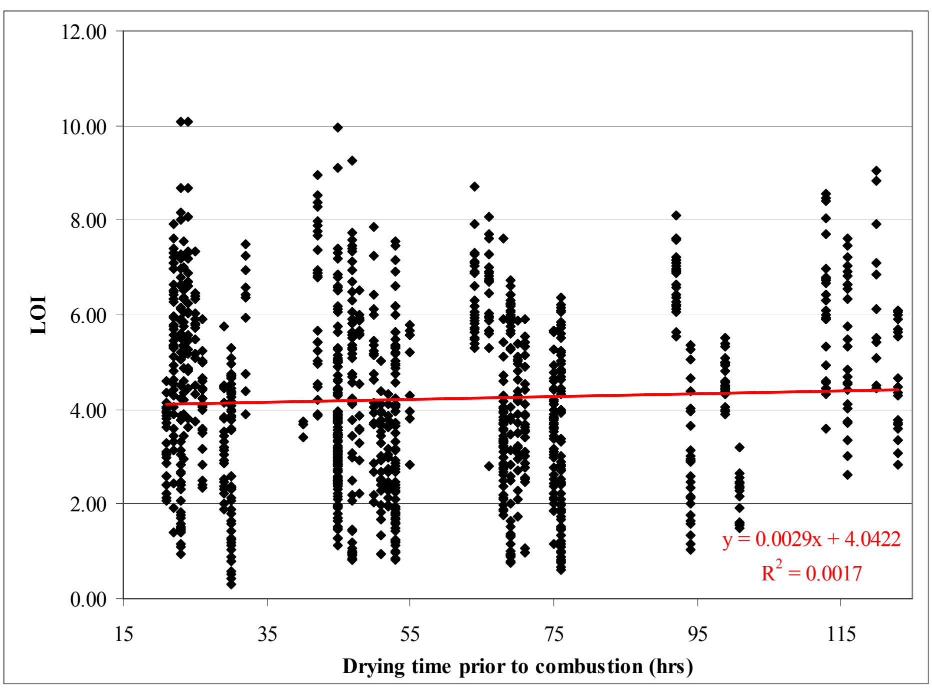

Figure 5.8: Sample LOI plotted over drying time. Each dot represents a sample. The red line represents the linear trendline.

Another approach was to average all samples with a given value for drying time and then plot the averages over drying time (figure 5.9). This resulted in a much clearer image. It also exhibited a much more pronounced relationship between drying time and LOI outcome.

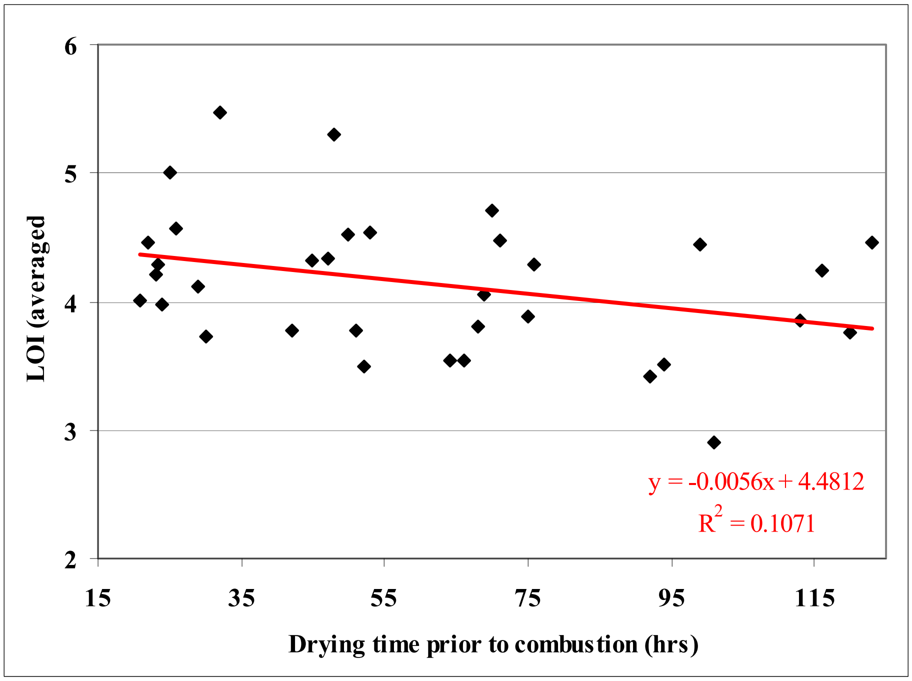

Figure 5.9: averaged LOI values plotted over drying time. Each dot represents all samples with a given drying time. The red line represents the linear trendline.

The LOI outcome decreases with drying time. Several possibilities arise that explain this phenomenon. Firstly, premature oxidation of samples during prolonged exposure results in lower organic carbon content before entering the furnace. Secondly, structural water in the samples' inorganic fraction may be evaporated during longer drying times. Under shorter drying times this water may be evaporated during furnace treatment (Heiri et al., 2001), therefore being incorporated in the LOI signal.

The outcome of these tests show that prolonged drying time may significantly influence LOI outcome. The average value of LOI results decreased by 0.7% of the total 4.0% (figure 5.9). The relative position of samples within a batch is not likely to have been changed due to prolonged drying. These findings are significant for the validity of outcomes of the various analyses presented in the rest this chapter.

5.3 Modeling sampling resolution

5.3.1 Sampling resolution model

This subparagraph describes the spreadsheet model that was used to simulate sampling at lower resolution. Original sampling took place at 1 cm resolution (chapter 4) which provides high levels of detail. It is an open question, what level detail is required for the study of flood records in channel fills. Sampling at lower resolution will reduce noise and dampen short lived excursions in the LOI curve. Without differentiating between the two, the spreadsheet model below attempted to simulate the data that would result from lower resolution sampling.

The model input consisted of the high resolution LOI data derived from each core. Next, a windowed average was applied at intervals of 2, 3, 4 and 5 cm. Each sample within a window was given equal weight in the average. The new average values were assigned a depth value equal to the average depth of the original samples.

In addition, the placement of each averaging window has several possibilities. For instance, one sampling at 3 cm resolution could start 1 cm earlier or later, resulting in a slightly different outcome. Therefore, a different model run was performed for each possible window interval. Two runs for the 2 cm resolution model, three possibilities for the 3 cm resolution model, and so on, resulting in 14 runs for each core, and a total of 56 runs.

The results of different resolution sampling - one run for each resolution – for the cores are displayed in figures 5.10 a-d. The reduction of variance with lower resolution, whether it is noise or signal, is visibly smoothed out in the averaging process. Note that for instance in core a, a large drop in LOI at 3.40 m is completely smoothed out at 5 cm resolution. The variance* of each curve is expressed in figure 5.10.

* variance (σ^2) = $\sum (a - \bar{a})^2 / N$

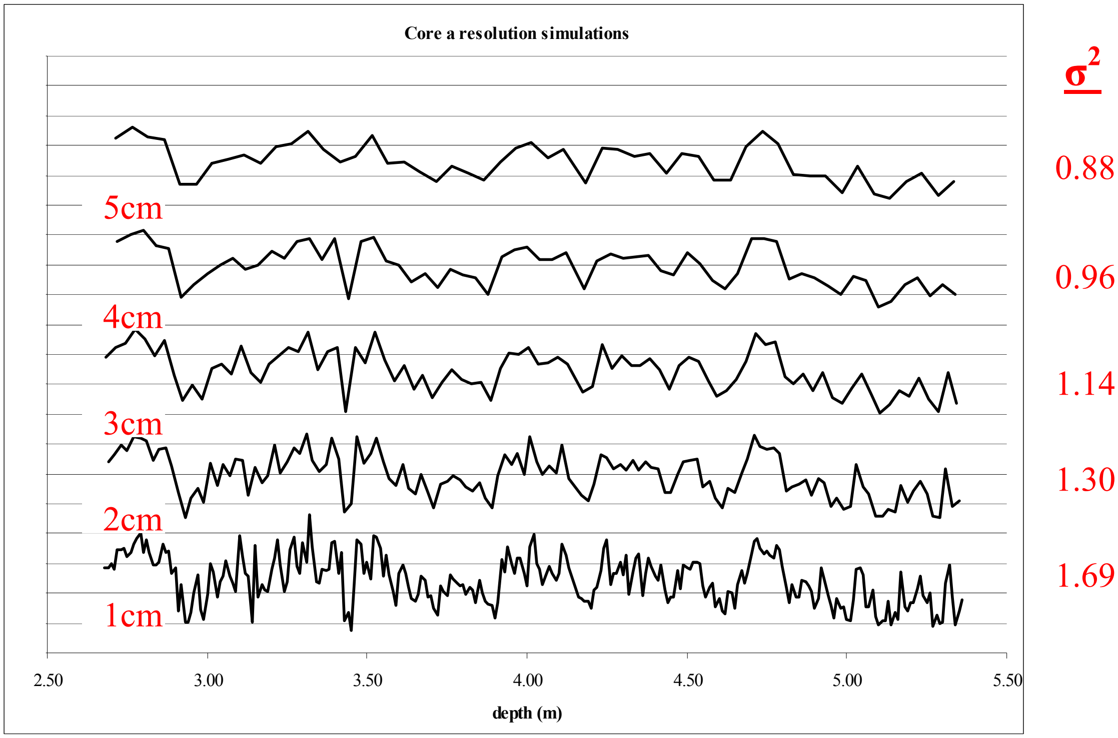

Figure 5.10a: core a LOI results at 1cm resolution, and simulated outcome of sampling at different sampling resolutions

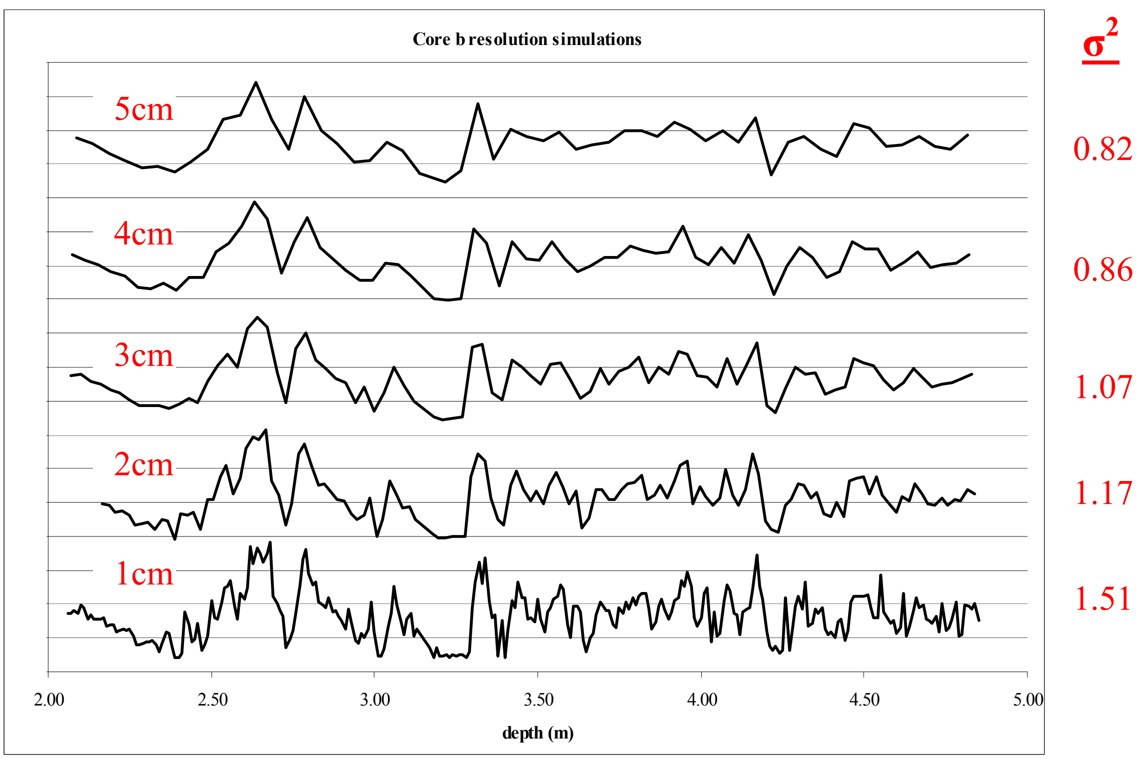

Figure 5.10b: core b LOI results at 1cm resolution, and simulated outcome of sampling at different sampling resolutions

5.3.2 Analyzing data: CPA

The simulation of different resolutions is just one step in investigating the effect of resolution on flood record research. The objective is to find out how a different resolution influences the outcome of the analysis. This subparagraph describes the procedure that was followed to perform the analyses on the cores at different resolution.

In this research, and even more so in the larger campaign, a very large amount of data is involved; 1267 LOI samples were concerned for this research alone. In the larger campaign more cores and more types of analysis will be involved. It is therefore essential to employ a standardized method of finding flood event signals within the analyzed data.

Statistical software was implemented to perform the analysis. The freeware program "Change Point Analysis" (CPA) was designed by Taylor (2000) to distinguish sudden trend breaks from the background trends – in this case long term trends in LOI level as a result of river activity and proximity.

CPA – the method applied by Taylor (2000) involves iterative cumulative sum charts (CUSUM) as described by Petitt (1980) to detect changes. Next, a process called bootstrapping (Efron and Tibshirani, 1993) is used to confirm changes and determine reliability and confidence intervals.

A CUSUM chart displays the cumulative sums of differences between values and the average. A sudden change in direction of the CUSUM indicates a sudden shift or change in the average.

Bootstrapping is a statistical method that basically performs the same analysis over and over using a different selection of the available data. If the outcome of the analysis is the same over many iterations, the outcome is more likely to be valid and can be determined with more confidence. A detailed explanation of these processes can be found in Taylor (2000)

The outcome of a CPA is given in graphs and tables. An example of a graph is displayed in figure 5.11. The LOI data is plotted and around it in turquoise a block representing the 95% confidence interval. A different block means the CPA has detected a change in the data. The red lines are conventional control chart boundaries, displayed for reference.

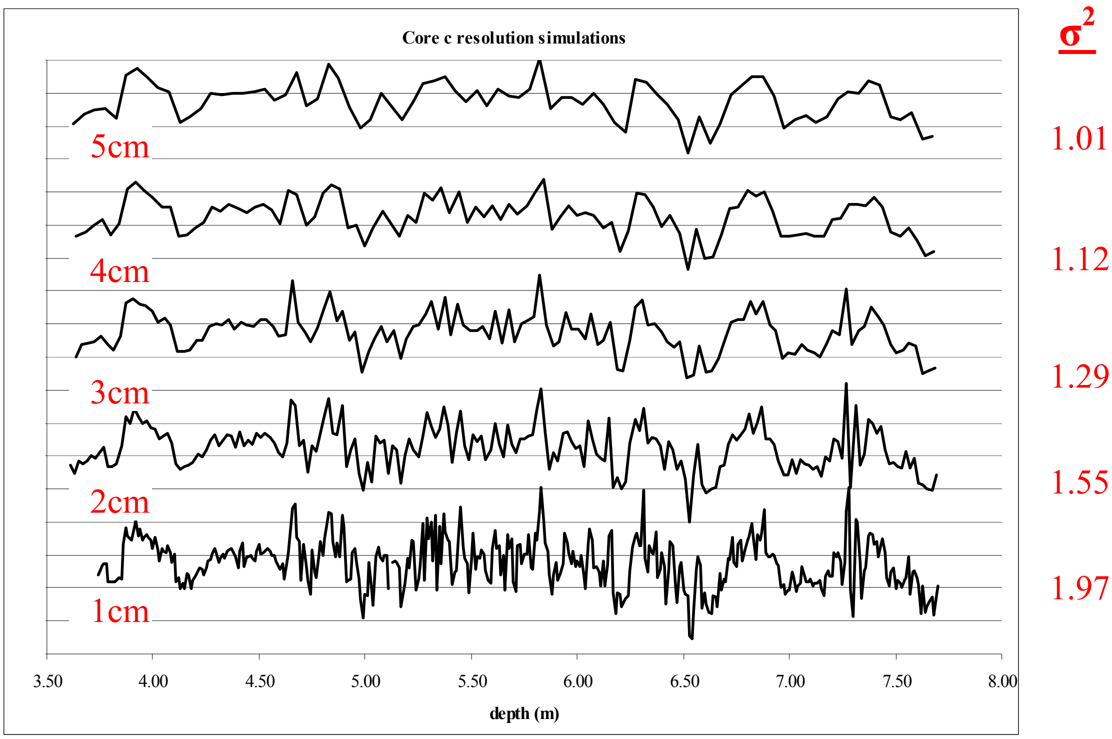

Figure 5.10c: core c LOI results at 1cm resolution, and simulated outcome of sampling at different sampling resolutions

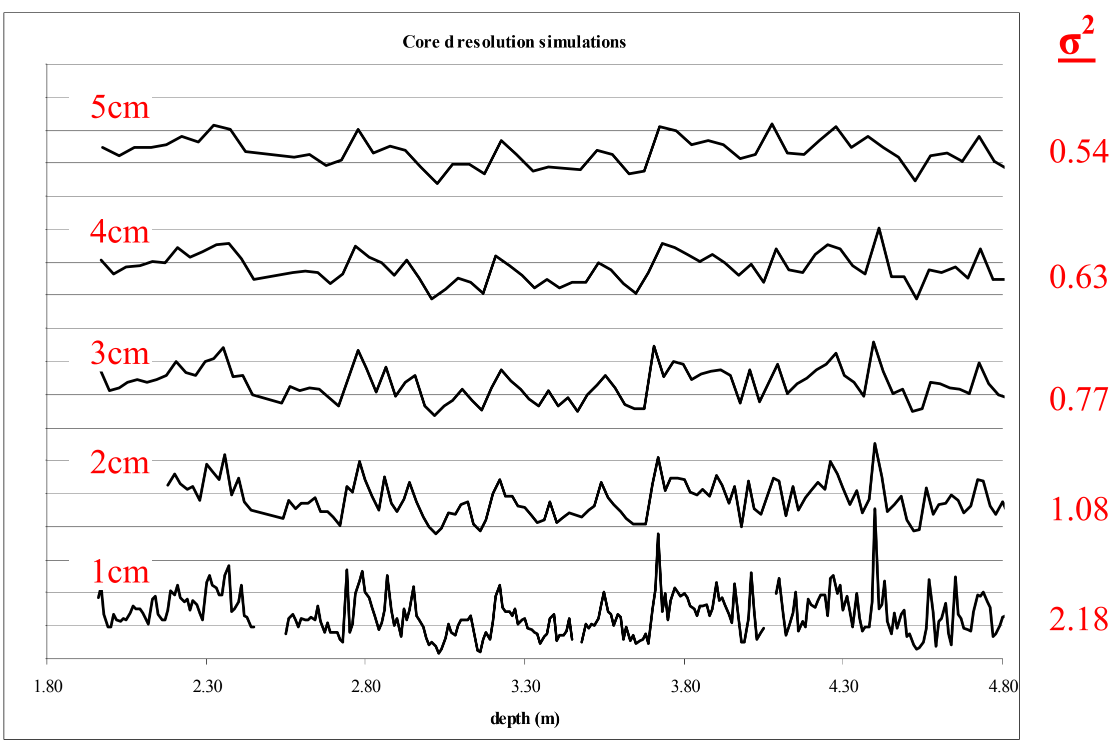

Figure 5.10d: core d LOI results at 1cm resolution, and simulated outcome of sampling at different sampling resolutions

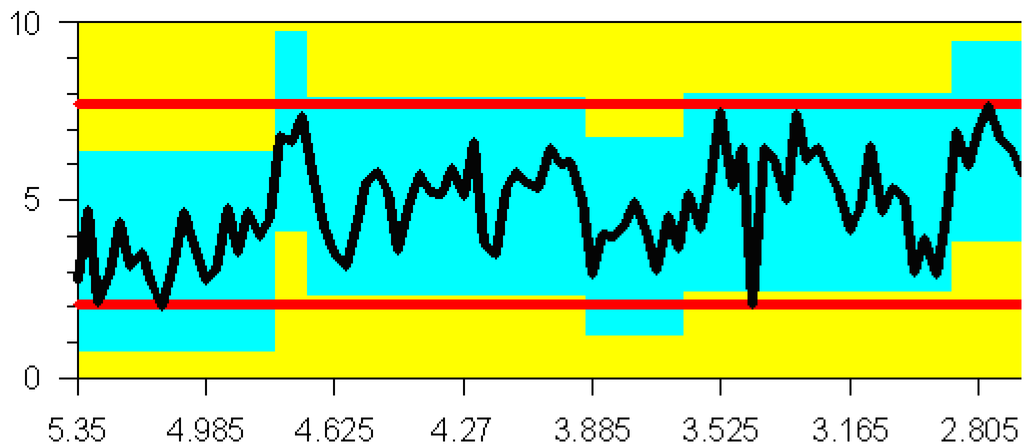

Figure 5.11: CPA graph of the results from core a).

From the table that accompanies the graph the numeric data concerning each point may be obtained. This graph provides information on exact coordinates of the change point, confidence intervals on the coordinates, the confidence level with which change occurred, and power of the change (i.e. magnitude of the trend break).

A CPA analysis was performed once on all cores at every resolution from 1-5cm. The outcome will be discussed in the following subparagraph.

5.3.3 Application of CPA on the LOI data

Based on the twenty runs (4 cores * 5 resolutions) an approach was adopted for the application of CPA on the LOI data in this research. Running the progam on high resolution data (1 and 2 cm resolutions) resulted in a “violation of assumptions” warning generated by the software. The automatic warning system detected indications that the data was not independent, i.e. that one value lying above the average was too likely to have a neighbour also above the average. This is not surpising, considering the nature of the data.

In addition to assumption violations, the program also invariably detected dozens of changes within each 1 cm resolution LOI record. Because it has no option to ignore smaller scale variations in large records, this proved to be impractical to work with.

In low resolution runs, CPA analysis often did not detect changes that were obvious to the trained eye. The reduced variability at lower resolution apparently caused the program to miss the trend breaks that are important. The compromise was to use the 3 cm resolution data. Data was subjected to a ‘ranked’ CPA analysis, which means that not the actual data was used for CPA but each sample’s rank value. This resulted in a satisfactory outcome for all four cores.

The CPA analysis rendered between 5 and 10 changes detected for each core at this resolution. Not all of these changes were feasible: some were too closely spaced for the area in between to actually represent a phase. Some had very low power levels assigned. A manual selection was made from all changes in each core, based on the placement, power level, and confidence level of each of the changes.

The adopted changes were then entered in the spreadsheet model for sampling resolution. For each interval between the changes, a linear trend line was calculated using the method of least squares. This line was considered the expected value for a given sample at that depth. An example of this is displayed in figure 5.12, for core a. The trend lines of all cores are displayed in appendix 3.

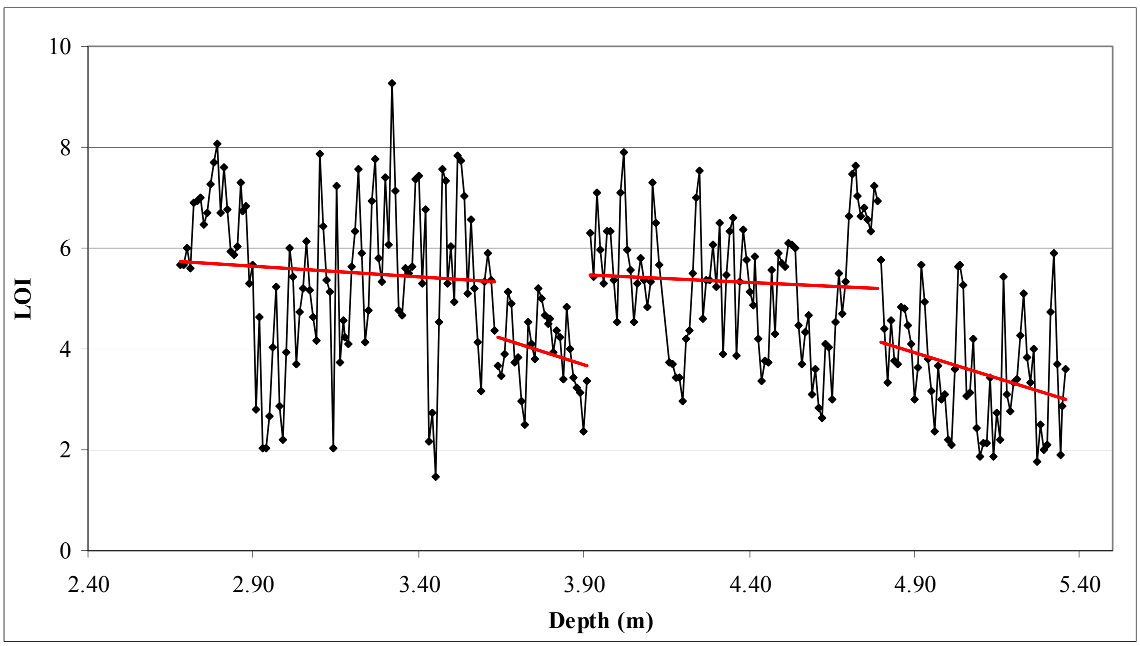

Figure 5.12: example of CPA induced trends plotted in the LOI data of core a. Trendlines are added in red.

The difference between the sample's expected value and the actual value, i.e. the sample's residue, was then calculated. This procedure was repeated for all the resolution runs in the spreadsheet model. The trend lines were applied to the appropriate depth intervals and residuals calculated.

To determine the effect of lower resolution sampling on flood event research, the difference in variability between resolutions must be measured. To this end, the standard deviation of the residuals of each interval was calculated. This standard deviation was then normalized after the standard deviation for that depth interval at 1 cm resolution. For example, in core a (figure 5.12) second interval ranges from 4.79 m to 3.92 m depth. The residuals on this interval at 1 cm resolution have a standard deviation of 1.28. At 3 cm resolution, the residuals on this interval for all three runs have an average standard deviation of 1.46, and when normalized after the 1 cm value, 1.14.

The results of the variability measurements and their bearing on resolution sampling will be discussed in the next chapter. The paragraph below is dedicated to the main question posed at the onset of this thesis, namely the possibility to cross correlate the cores.

5.4 Wiggle matching data from adjacent cores

5.4.1 Wiggle matching model

The method of wiggle matching postulates that changes in one record are reflected in other records of similar recording setting, and continuity of records of the same age. For example, a set of tree rings in one tree matches tree ring records of surrounding trees in the area, as exploited in dendrochronology.

During fieldwork, great natural lithological variation was observed. For the purpose of cross correlating different cores this inter core variability is considered ‘noise’. The wiggle matching model tried to eliminate small scale variations that originated from local influencing factors or possible measurement errors. Instead, the focus of the research was on larger events, represented by distinct, multi-cm excursions in the LOI curve. In order to do so more easily, smaller variations were eliminated from the data. This was accomplished by first treating the LOI data with a running average window. Each sample value was smoothed out by its neighboring values. This allowed short lived extremes to lose power compared to larger trends, which are relatively unaffected. This smoothened data was used to initially wiggle match the LOI curves of separate cores. After matching the large trends, the match was fine tuned using the original data.

Because of its central position and the fact that it is the longest record used in this research, core c was used as the central piece. Cores a and d were matched to this core. Core b, which is placed closest to core a, was matched to its immediate neighbor. This was done mainly because this core is different from the other cores in the sense that it is positioned on the ‘outside’ of the residual channel, instead of at the deepest point.

In a spreadsheet, the cores are matched manually, working from bottom to top. The bottom of each core is the channel lag, which represents the only marker that these cores have in common. The LOI value of each sample is attached to a certain depth. For wiggle matching, the depth of each sample is made variable, as opposed to its original solid depth scale with 1 cm resolution.

Each sample is assigned a depth value which depends on the value of the sample directly below, and a factor x. The default setting for 'x' is 1. This renders the original dataset. Changing the value of 'x' for a given sample changes the depth of this sample and all samples above it, but not that of all the - previously wiggle matched - samples below. By adjusting the value of 'x', the occurrence of extreme values in the record may be postponed or advanced to overlap with the occurrence of its core c equivalent, if any.

5.4.2 Wiggle matching results

The different cores corresponded to each other remarkably well. Sedimentation rates between cores diverged markedly at different times – this will be explained further in the next chapter. Nevertheless, any excursion in one core was typically reflected by similar excursion in most cores, down to the single centimeter. This made wiggle matching the cores elaborate, but also more accurate.

As an example, the match between cores c and a is displayed below (figure 5.13). The figure shows core c on its original depth scale, and core a after depth has been adapted in the wiggle matching model. Tick marks are added to visualize the adaptations made to the core a depth scale. Concentrated tick marks indicate concentration of core a LOI data.

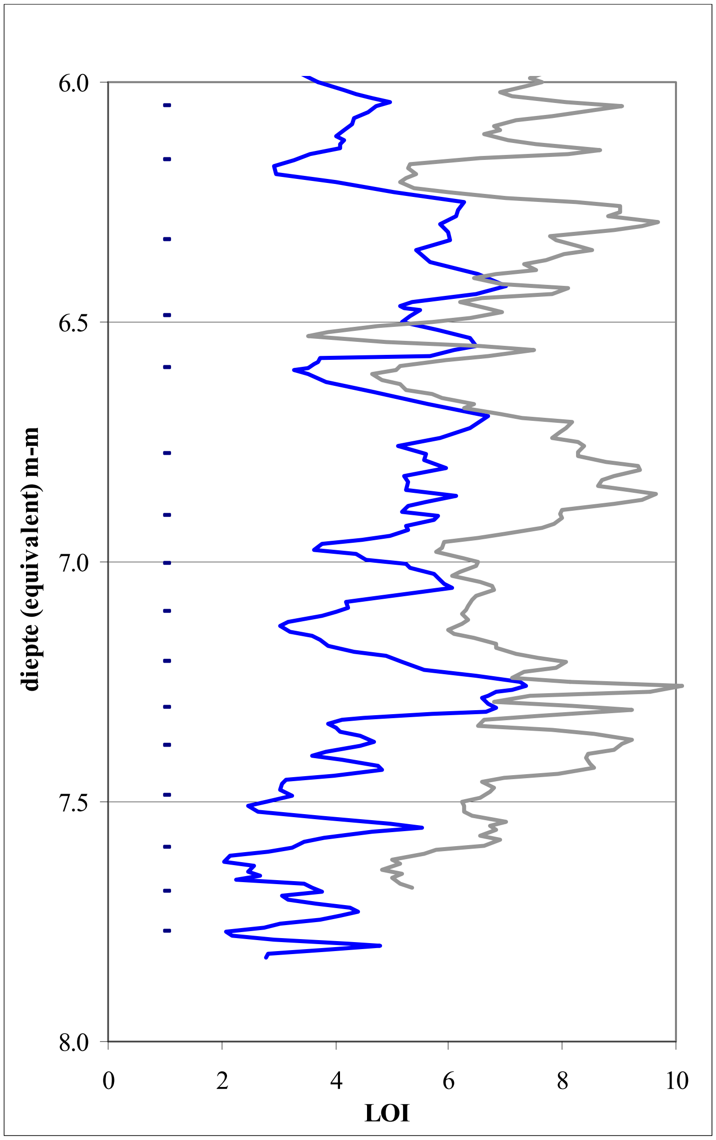

Figure 5.13: wiggle match example. To the left partial LOI results for core a, to the right partial results for core c. The tick marks on the right that indicate concentration and dilation of core a data.

Note that, in figure 5.13, most exursions in one curve are reflected in the other as well. For instance, notice the steep drop in LOI in both cores around 6.25 m (equivalent) depth. However, it is also clear that the magnitude of the excursion is rarely the same. For instance, notice the 10 cm wide excursion in core a at 7 m equivalent depth, while in core c, this is almost absent.

It was possible to wiggle match the other cores to cores a and c in a similar way. This resulted in the overview illustration of the wiggle matches presented in the next chapter. There, the matched core data will be used to draw conclusions from the outcome.

6. Discussion of results

The previous chapters cover the research's facets of data accumulation, data analysis, and outcomes. This chapter discusses the products of these steps and their relevance to flood event research, organized in separate paragraphs. First, the findings concerning the paleogeographic setting of the residual channel are related. Pollen count results, transects, and other findings; what can be concluded about the Waalsprong area based on this information? Second, the significance of the analyses described in the previous chapter is assessed. Has the approach taken produced the desired results? What factors may have influenced these results? The applied procedures are evaluated.

6.1 Paleogeographic setting of the Waalsprong area

This paragraph covers the reconstruction of the residual channel and its paleoenvironment. The reconstruction is not extensive because it is not the focus of this thesis. Understanding the background of the data does help to explain variability that the data exhibits. Moreover, the techniques employed in this thesis and discussed in this chapter ultimately serve to better understand the paleoenvironment in terms of river activity and its influence on the surroundings.

6.1.1 Pollen data and archeology

The pollen data returned a general sketch of the sedimentary environment of the residual channel. Two important conclusions can be drawn, although the report emphasizes the uncertainty with which it can make statements. The first conclusion is that the species' composition of the pollen in the channel fill reflected by the pollen data indicates an environment of slow but continuous flow. This means that the residual channel was never completely cut off from the main channel and remained within the abandoning stage (see chapter 2) until completely filled in. More evidence regarding flow conditions in the residual channel is presented in the next subparagraphs.

The second conclusion concerns the age of the channel fill. The species' composition pointed towards Subboreal-Subatlantic conditions. It concludes this is a "relatively quickly filled residual channel, with materials deposited between ~3000 yrs BP (upper Subboreal) and ~2700 yrs BP (onset Subatlantic)" The report stresses the complicating factors, such as continued flow bringing in allochtonous materials.

Preliminary archeological estimates from excavations at the fieldwork site indicate that around roman times (~2100 yrs BP), the residual channel still supplied surrounding inhabitants and cattle with open water, still or flowing.

6.1.2 Fieldwork data, transects and surroundings

The fieldwork campaign described in chapter 3 covered the area directly surrounding the residual channel treated by this thesis, and beyond. This subparagraph considers this in the perspective of findings from corings performed outside the described fieldwork area.

According to Lodiers (2008), this channel flowed from north to south. In a later stage of the Ressen system, the deposits north of transect 1 were replaced by younger. A detailed study of the AHN (figure 6.1) however shows that a coring site to the northeast of this channel may be connected. Pollen data from a core taken there (UTM 187200, 432 400) indicate similar age and infilling conditions. This opens up new questions about the origin and period of activity of this paleochannel.

At cross section 1 (figure 6.1), the residual channel curves slightly towards the south. Supposing flow from the northeast, concentration of flow at the outer bend (northwest of the transect) is expected. Cross section 1 (appendix 1 a) indeed reveals the deepest point of the channel at the northwest end.

At the location of core c (figure 6.1), the channel changes direction from northeast-southwest to northwest-southeast. The cross section in figure 3.3 (also, appendix 1 b) shows the deepest part in the western end of the channel, consistent with the expected concentration of flow in the outer bend. At cross section 2, the channel has no such prevalent distribution of sediments (appendix 1 c). The channel seems to be in this area (figure 6.1), and cannot be traced further south.

The cross sections further exhibit signs of a small reactivation phase (figure 3.3, appendix 1 a), that falls outside the scope of this thesis. The shape of the channel fill, with steep banks at the outer bend and steady sedimentation at the inner bend, particularly resembles scenario A, as described in chapter 2. This scenario is further discussed in the next subparagraph.

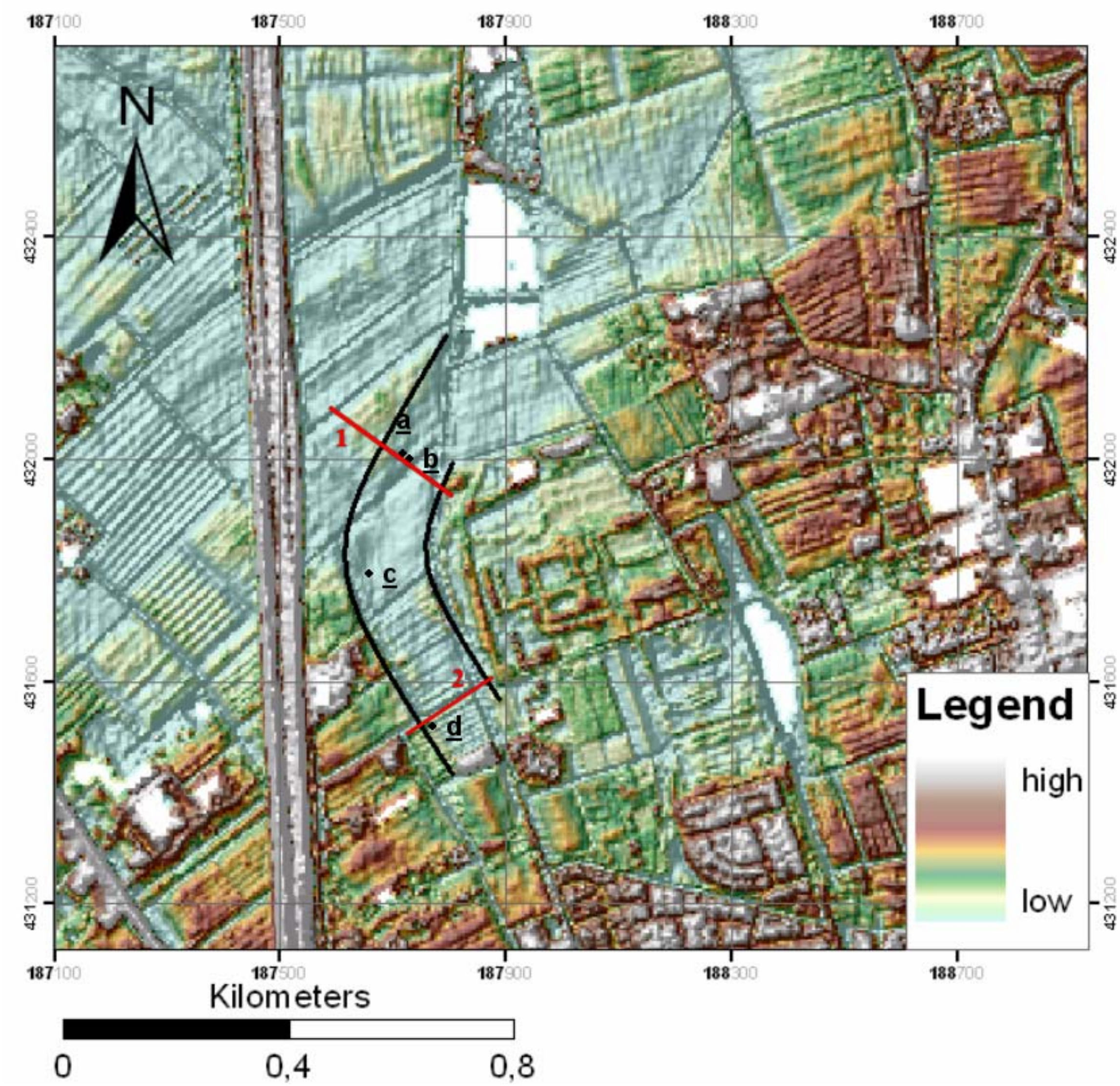

Figure 6.1: copy of figure 3.4. Black lines underline the limits of the paleochannel. Coring locations are indicated with black dots, accompanied by an identifying letter. Red lines indicate cross sections. North of transect 1 (north), the depression representing the possible residual channel can be traced to the northeast.

6.1.3 Core data

The data extracted from the cores provides more clues about the paleoenvironment of the residual channel. In the first place, the pollen data indicated continued flow during the infilling. This is consistent with the relatively low levels of organic matter that were found in the channel fill. The continued flow restricted peat formation. Furthermore, it provided input of clastic materials in the form of clay even during periods of low river activity.

Also, the sudden transition from channel lag deposits to fine clastics found in the cores indicates a quick transition to slower flow conditions. No plug bar deposits were found in the corings indicating that the avulsion point was further upstream.

Additionally, the inter-core relationship provided by the wiggle matched cores can provide details of interest. In figure 6.2 the complete wiggle match is displayed for all four cores. The first detail worth mentioning is that the curve of core d is matched completely to the bottom of core c, although a channel lag deposit was not found in core d. It is therefore unlikely that the residual channel extends any deeper than what was extracted during this fieldwork. The deposits at the bottom of the channel at this point contain sand, in contrast to the other cores.

Another detail is the deepest core, core c, is also filled the quickest. Figure 6.2 shows that the same record encompasses more depth at this location than in cores a and d. Similarly, core b, located just at the inner bend of the deepest point of the channel (figure 6.1), is filled up slightly slower than core a.

This seems to point at the process of channel shallowing, as described chapter 2. The location away from the abandoning point and at a bend in the channel points at scenario A or C, described by IJmker (2008). Especially the cores from at transect 1 seem to point at scenario A, with slightly higher sedimentation rates at the deepest part of the channel (figure 2.1)

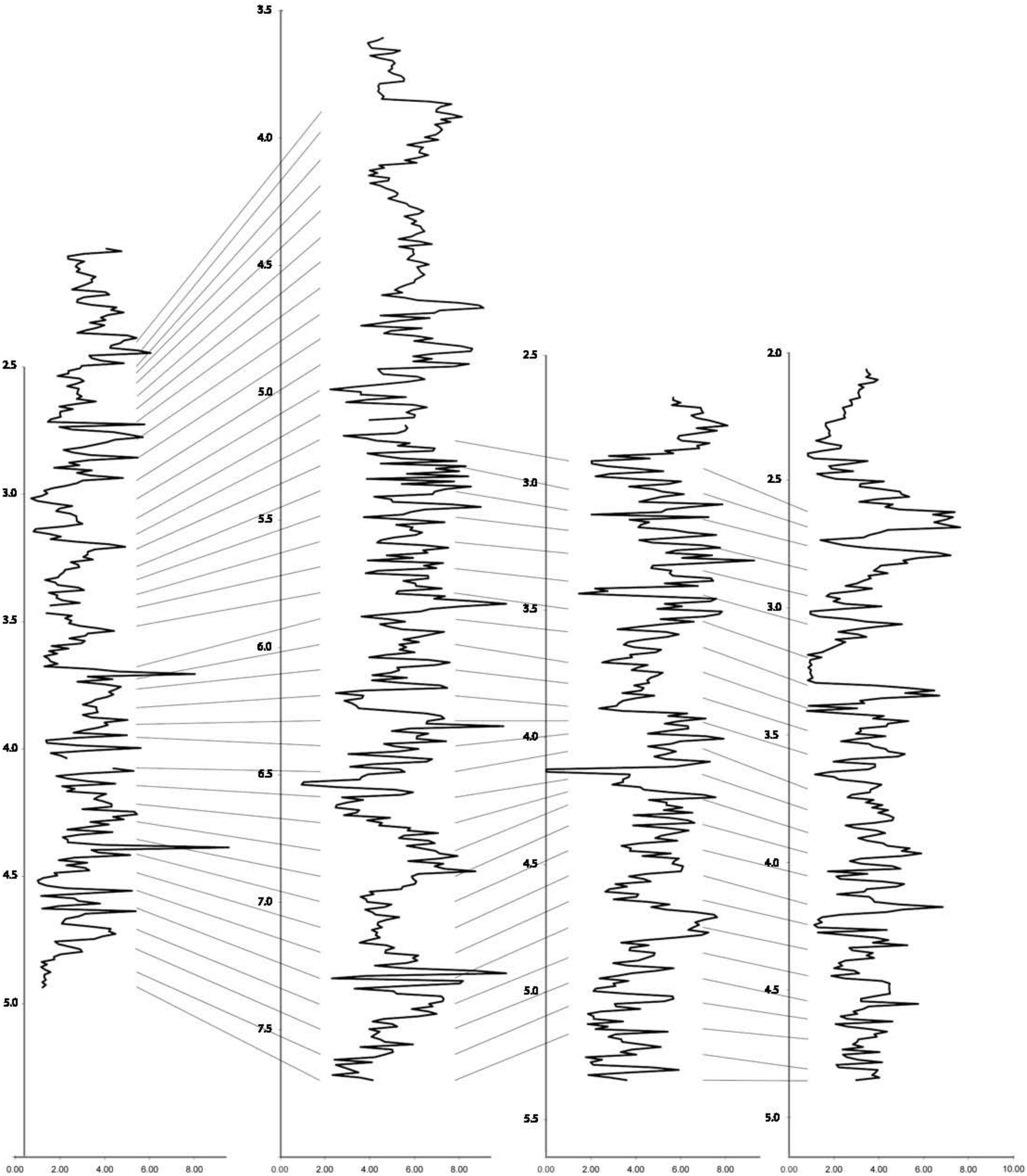

Figure 6.2: complete wiggle match of all four cores. From left to right: core d, core c, core a, core b. Lines are drawn between equivalent depths. Each core is on a separate depth scale.

6.1.4 Summary of paleogeographic setting

The channel explored in this research was abandoned in the late Subboreal (~3000 yrs BP) based on pollen records. It was filled in relatively fast, and flow never completely stopped until the infilling was complete. There are indications that the residual channel can be traced towards the NE, contrary to the mapping results of Lodiers (2008).

The deepest point of the channel was found at the outer bend at the location of cores a, b and c, while at the location of core d it was more symmetrical. Sedimentation rates were highest at the deeper points in the channel, indicating channel shallowing as an important process. Scenario A, as described by IJmker (2008 – MSc thesis), best describes the coring results with steep outer bends and steady sedimentation on the inner bends.

6.2 Analysis of LOI data from flood event records

This paragraph discusses the validity and significance of the methods that this research has employed. In the following subparagraphs, the outcome of the reliability tests is considered. Next, the model used for simulating sampling at different resolutions is discussed. Then, the comparability of the used cores is argued.

6.2.1 Reliability of LOI data

The tests that were run on furnace position, carbonate content, and drying time were conclusive. Little significant influences were found, except for a generally lower LOI result for samples with long drying times. Drying times could be reduced by sampling less at a time, so that less samples are queued. This has drawbacks: the cores have to be reopened multiple times to completely sample them. This requires more time and increases the risk of damaging the core. When sampling at lower resolution, a complete core may be sampled and processed without queuing samples; 2 cm resolution sampling results in 50 samples (= 2 batches * 25 samples) per core, which can be processed within one day. Another option is enlarging furnace capacity to increase processing speed and reduce queuing time.

6.2.2 Sampling resolution

The spread sheet model investigating the influence of sampling resolution on data quality performed admirably. The resulting reduction in total variability however consists both of a reduction in noise, as well as a reduction in signal. The decay of potential information is visualized in figures 5.10 a-d. However, the calculated reduction of variance is also portrayed below (figures 6.3 a-d)

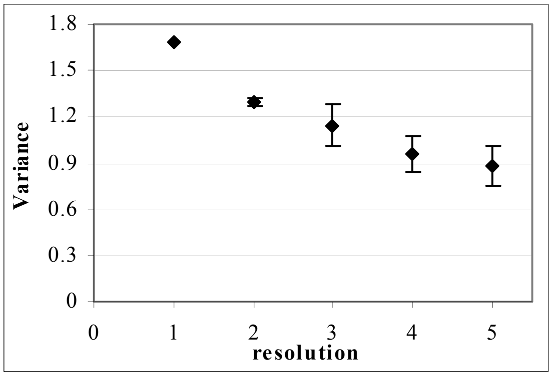

Figure 6.3a: reduction of variance in core a at (simulated) lower resolutions

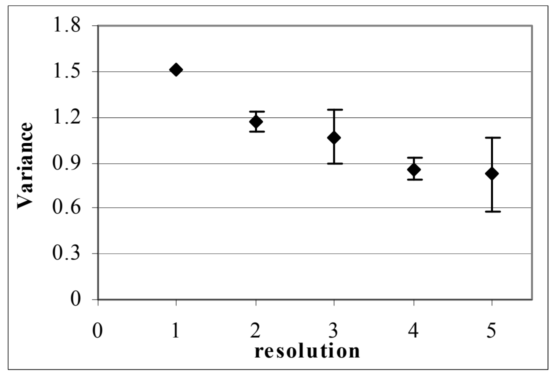

Figure 6.3b: the same as 6.3a, but for core b

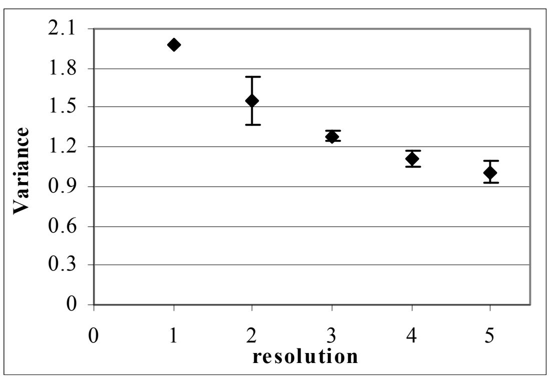

Figure 6.3c: the same as 6.3a, but for core c

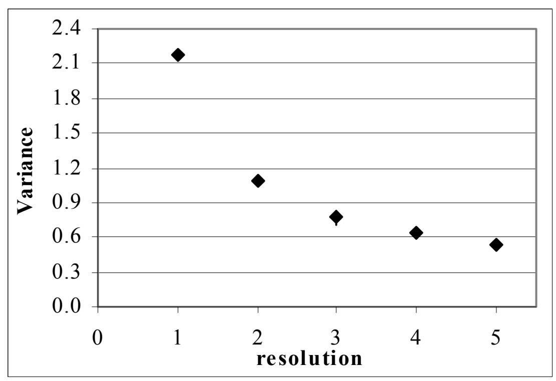

Figure 6.3d: the same as 6.3a, but for core d

The dots in the image are the average standard deviation of residuals at a given resolution. The error bars are based on variation within different versions of one resolution, as described in chapter 5. The images above show a sharp decrease in variance occurs when data is simulated in lower resolutions. The variance is reduced, by a factor 2 or more in all cores, between 1 cm and 5 cm resolution data.

The loss of signal, especially the signal from larger events, is modest in the higher resolution runs (figures 5.10 a-d). At 4 and 5 cm resolutions, even the more important events lose power in these graphs (figure 5.10 a). A three centimeter sampling resolution is considered optimal for these cores. This is put in perspective when considering the length of the records. In the case of longer cores such as with Minderhoud (2008), these contain more variation, and encompass more and larger events. The low resolution options described in this thesis might be just right for such a record. In case the low resolution modeling needs to be extended or repeated, the model used is easily adapted to the required settings.

6.2.3 Comparability of cores

The displayed wiggle matches (figure 5.13; figure 6.2) illustrate that LOI data exhibits similar responses in closely spaced cores. This supports the practice of regional flood event reconstruction based on cross correlating different flood records.

The only marker that was available – the channel lag deposits – proved to be valuable, but inaccurate. The LOI record of core a, which was wiggle matched to cores b and c, was found to extend 10-20cm further down than the other cores. When cross correlating cores from different channels, different factors will start playing a role. More emphasis is put on markers between cores, with a preference for multiple markers providing a jumpstart for the wiggle match. Also, local influences will cause larger differences between separate channels than within one residual channel. A good understanding of the paleoenvironment will be vital in explaining divergent behaviour of proxy data from equivalent events in different cores.

The approach of smoothing the data before wiggle matching was found to improve the overview over the data and made wiggle matching easier and quicker. Reduction of noise helps to create overview of the record and allows focus on the most important, long term influences first. Fine tuning smaller events is much easier and more accurate if the depth model is already roughly correct.

6.2.4 Summary of methodological effectiveness

The tests concerning LOI reliability returned little factors of significant influence on LOI outcomes. Possible influence from long drying time is easily countered by queuing less samples or increasing furnace capacity.

The modeling of lower sampling resolutions produced clear and quantifiable results. These are relative to the length of the record, however; in a longer record, a lower resolution sampling procedure may give better results.

The LOI results derived from the cores corresponded to each other well and were easily wiggle matched. The approach of smoothing noise by a running average window facilitates the process. For wiggle matching cores from different sites, this approach is recommended. Multiple markers between cores are preferred to commence wiggle matching. Inter-site comparability of cores will suffer from greater influence by local factors.

7. Conclusions

The channel explored in this research was abandoned in the late Subboreal (~3000 yrs BP) based on pollen records. It was filled in relatively fast, and flow never completely stopped until the infilling was complete. There are indications that the residual channel deposits continue towards the NE, contrary to the mapping results of Lodiers (2008).

The deepest point of the channel was found at the outer bend in transects 1 and the Cohen and Heunks transect. It lacked preference at transect 2. Sedimentation rates were highest at the deeper points in the channel, indicating channel shallowing as an important process. Scenario A, as described by IJmker (2008 – MSc thesis), best describes the coring results with steep outer bends and steady sedimentation on the inner bends.

The tests concerning LOI reliability returned little factors of significant influence on LOI outcomes. Plant remains and other disturbances were found to have negligible influence. Possible influence may come from long drying time prior to combustion. This is easily countered by queuing less samples or increasing furnace capacity.

The modeling of lower sampling resolutions indicated that sampling at 3 cm resolution would yield satisfactory results at less time investment than the original 1 cm resolution sampling. The optimal resolution is relative to the length of the record, however. In a longer record containing more and larger events, a lower resolution sampling procedure may still provide information on the large flood events.

The LOI results derived from the cores corresponded to each other well and were easily wiggle matched. This supports the practice of regional flood event correlation. The approach of smoothing the curve with a running average window facilitated the process of wiggle matching. For wiggle matching cores from different sites, this approach is recommended as well. The channel lag was not a reliable marker for wiggle matching the core. Multiple markers between cores are preferred to commence wiggle matching. Inter-site comparability of cores will suffer from greater influence by local factors.

This research confirmed the application of LOI as a proxy for flood event research. The data was clear and provided excellent opportunities for flood event identification and correlation of cores.

8. Suggestions for future channel fill research

During the research, a number of issues were encountered that were not addressed in this thesis. They fall outside the scope of this research or the current procedure could be improved upon. This chapter deals with suggestions of the author for future research on channel fills based upon the experience of this study. The first paragraph reflects upon the used coring material. Then two paragraphs concerned with the computerized analyses are inserted; one containing suggestions on sampling resolution, the other on wiggle matching. Finally, some miscellaneous suggestions are added.

8.1 Coring

The two methods used to extract cores, described in chapter 3, were the Begemann mechanical corer, and the Bohncke piston corer. Both these corers have advantages and drawbacks. The Begemann corer delivers undisturbed, well preserved core material from surface to channel lag. It is expensive, however, and cannot be deployed everywhere. The Bohncke corer is inexpensive and can be deployed everywhere, but the material is more likely to be damaged during the many steps required to extract a core.

This research found that data quality did not suffer much from the multitude of acts of the Bohncke corer. Despite signs of disturbance by the corer (appendix 2 d), the LOI outcome was closely related to that of the other cores. In more sandy sections, disturbances were abundant and will have reduced data quality. The use of the Bohncke corer is recommended for future channel fill research based on these findings.

8.2 Sampling resolution

The modeling of sampling resolution results was explorative. The use of the freeware program CPA (Taylor, 2000) worked out, but in fact the intended function of the program is quite different from the way it was employed here. The program functions best in a relatively stable dataset, where an isolated event changes the direction of the curve.

The natural variability of the data in these records was too great for the program to handle properly. This resulted in numerous 'detected changes' which had to be manually discarded.

This will be less of a problem in larger datasets (deeper cores), for several reasons. Firstly, larger datasets will exhibit more large events that have great impact on the curve and are more easily picked up by the program. Secondly, long term trends will emerge above the level of noise as well. Especially when sampling at lower resolution or when smoothing the data, the noise will be smoothed while signals from large events persist. This will assist the software to separate actual events from the background variation.

A note on actual sampling resolution is that, although it is clear that higher resolution does not necessarily produce better results, it is difficult to find the optimal sampling strategy for an entire core. A different option is to take on an adaptable sampling strategy, based on visual assessment of the core material. In case of e.g. sub-centimeter laminations in the core, a locally higher resolution may be adopted.

8.3 Wiggle matching

The approach of smoothing data and reviewing long term trends first was successful in this research. Especially when records stem from more distal environments, trends found in one record may be entirely local in origin. E.g. proximity of the active system influences background level of sedimentation and impact of flood events (Middelkoop, 1997). The trends resulting from changes in proximity are not likely to be reflected in other records. A good understanding of the paleoenvironment of the record is therefore a necessity in establishing inter-site relations between records.

The use of longer records (deeper cores) has advantages for wiggle matching as well. Improved noise reduction is made possible, which facilitates comparison. Also inclusion of more and more important events give correlation with a master record a better chance of success as there is a larger overlap with such a master record.

The model for wiggle matching the four cores in this research was relatively simple. Because there was only a limited amount of data, manual adjustments were sufficient. In case of longer datasets, preliminary interpolation between markers and datings may be performed by statistical software, such as *Analyseries* (Paillard et al, 1996). This could facilitate comparison of a record to a master dataset with a compilation of records.

8.4 Miscellaneous suggestions

The residual channel that was explored in this research was considered at the start to be disconnected from its environment by erosion from later river systems. Information given in chapter 6 suggests that another coring site to the northeast of the fieldwork area is nonetheless connected to this channel. Investigating this connection could improve the understanding of the Ressen channel belt complex. Speculatively, this connection could extend further NE than location 13 alone.

Building on the relative sedimentation rates of the cores, presented in figure 6.2 of this research, and the study from IJmker (2008), future research may generate more information about channel fills. Ultimately, this may result in detailed understanding of variables responsible for the architecture of a local channel fill. A challenge could be to draft a theory of aggegrate sedimentation, incorporating factors such as flow condtions, distance to abandoning point, active system sediment load, an error factor etc. to predict channel fill architecture based on known variables.

A final subject of interest is to find exactly the influence of carbonates in channel fill material on LOI. The samples treated in this thesis contained limited amounts of carbonates. Carbonate influence may become more important in channel fill research to come.

References

Publications

De Bakker, H., and Schelling, J., 1966, *Systeem van Bodemclassificatie voor Nederland; de Hogere Niveaus*, Pudoc, Wageningen

Berendsen, H.J.A., 2004, *De vorming van het land – Inleiding in de geologie en geomorfologie*. Assen: Van Gorcum, 4e geheel herziene druk, 410 p.

Berendsen, H.J.A. and Stouthamer, E., 2001, *Palaeogeographic development of the Rhine-Meuse delta.* Assen: Van Gorcum, 268 p.

Brown, M., and Lowe, D., 2007, *Automatic Panoramic Image Stitching using Invariant Features*. International Journal of Computer Vision, 74(1), pages 59-73

Cohen, K.M. and Lodder, Q.J., 2007, *Paleogeografie en veiligheid tegen overstromen: de bruikbaarheid van inzichten in de ontwikkeling van de Nederlandse delta in de laatste 5000 jaar voor het kwantitatief begrenzen van overstromingsmagnitudes en –frequenties*. RIZA Rapport 2007.016., Lelystad: RIZA.

Dean, W.E. Jr., 1974, *Determination of carbonate and organic matter in calcareous sediments and sedimentary rocks by loss on ignition: Comparison with other methods*. Journal of Sedimentary Petrology. 44: 242-248

Duijkers, M.C.H., 2009, *Lateglacial climate change and chronology at Lurga, western Ireland; derived from multiproxy and microtephra analysis*. MSc Thesis Physical Geography, Utrecht University. Unpublished.

Heiri, O., Lotter, A.F., and Lemcke, G., 2001, *Loss on ignition as a method for estimating organic and carbonate content in sediments: reproducibility and comparability of results*. Journal of Paleolimnology 25: 101-110.

Efron, B., and Tibshirani, R., 1993, *An introduction to the Bootstrap*, Chapman and Hall, New York

Hoekstra, J., 2008, *The fall of the Schenkenschanz: Geomorphological development of the evolution of the Waal-Nederrijn bifurcation in the river Rhine, since 1550 AD*. MSc Thesis Physical Geography, Utrecht University. Unpublished.

IJmker, J.M., 2008, *Development and infilling of the Tolkamer Old Rhine residual channel in the last 450 years (Rhine-Meuse delta, The Netherlands).* MSc Thesis Physical Geography, Utrecht University. Unpublished.

Lodiers, S., 2008, *De oorsprong van de Waalsprong*. MSc Thesis Physical Geography, Utrecht University. Unpublished.

Middelkoop, H., 1997, *Embanked floodplains in the Netherlands : geomorphological evolution over various time scales.* Utrecht: Koninklijk Nederlands Aardrijkskundig Genootschap. 341 pp.

Minderhoud, P.S.J., 2009, *5000 years Rhine flooding as recorded in a paleochannel near Rheinberg (Germany)*. BSc Thesis Physical Geography, Utrecht University. Unpublished.

Paillard, D., Labeyrie, L., and. Yiou, P., 1996. *Macintosh program performs time-series analysis*. *Eos,* 77:379

Petersen, W.G., Chesters, G., and Lee, G.B., 1966, *quantitative determination of calcite and dolomite in soils*. Journal of soil science, 17:329-338

Pettitt, A. N. 1980, *A simple cumulative sum type statistic for the change-point problem with zero-one observations,* Biometrika, 67 1, 79-84.

Stouthamer, E., 2001, *Holocene avulsions in the Rhine-Meuse delta, The Netherlands*. Netherlands Geographical Studies 283, 211 pp.

Taylor, W., 2000, *Change-Point Analyzer 2.0 shareware program,* Taylor Enterprises, Libertyville, Illinois. Web: http://www.variation.com/cpa

Van de Meene, E.A., J. Van der Staay and Hock, T.L., (1979), *The Van der Staay suction-corer - a simple apparatus for drilling in sand below groundwater table*. Rijks Geologische Dienst, Haarlem: 1-15.

Ven, G.P. van de, 1976, *Aan de wieg van Rijkswaterstaat; Wordingsgeschiedenis van het Pannerdens kanaal*. Zutphen: De Walburg Pers.

Institutes

Coring methods:
http://www.geo.uu.nl/fg/palaeogeography/LLGDatabase/coringmethods

Deltares, 2009, *Begemann continue steekboring voor archeologisch onderzoek*, digital publication, www.deltares.nl

NIOZ-AVAATECH. *XRF-corescanner*: www.nioz.nl

NOAA free software list: http://www.ncdc.noaa.gov/paleo/softlib/softlib.html

RAAP, 2001. *RAAP-brief 2001-3549, kaartbijlage 1*, Amsterdam

Rijkswaterstaat-AGI, 2005. *AHN: Actueel Hoogtebestand Nederland*. www.ahn.nl

TNO Toegepast Natuur-wetenschappelijk Onderzoek www.TNO.nl

Acknowledgements

This research has been rightfully been the most challenging and engaging work of my MSc curriculum. Due to the early stage that channel fill research is in, finding the best approach is not always straightforward. In fact, to speak with the words of my direct supervisor, drs. Willem Toonen, it often 'involves acts of pioneering'.

Never was this more clear than when we both were clad in rubber suits, carrying loads of coring equipment through waist deep marshes at 30 °C. But apart from fieldwork experiences, which I will remember with fondness, I would like to thank Willem for his support, his explanations and helpful suggestions during the work in the laboratory and behind the computer. On top of that, your preparations for the fieldwork ensured that I slept in a solid house every night after a fieldwork day. Thank you!

More thanks go to my supervisor, dr. Kim Cohen, for guiding me on this subject, for your company at difficult coring sites, but mostly for your generous and very helpful suggestions on my research as well as writing this thesis.

My gratitude extends to all occasional others who helped make this research work: dr. Wim Hoek for demonstrating the sometimes 'difficult' workings of the Bohncke corer, and instructions on laboratory practice. The Begemann coring team for their clear explanation of the complicated device as well as their quick and professional work.

Mostly, I owe a debt of gratitude to my friends Jeroen Gout and Mark Opfer-Ruting, who helped out with the extraction of the Bohncke cores during fieldwork. You took the accompanying hardship for granted and became 'Bohncke core veterans' in one day. Thank you very much for your willingness to help.